The distinctive electrowetting properties of ITIES

2007 J. Phys.: Condens. Matter 19 375113

(http://iopscience.iop.org/0953-8984/19/37/375113)

IOP PUBLISHING JOURNAL OF PHYSICS: CONDENSED MATTER

J. Phys.: Condens. Matter **19** (2007) 375113 (29pp) doi:10.1088/0953-8984/19/37/375113

The distinctive electrowetting properties of ITIES

Charles W Monroe[1], **Michael Urbakh**[2] **and Alexei A Kornyshev**[1]

[1] Department of Chemistry, Imperial College London, South Kensington Campus, London SW7 2AZ, UK
[2] School of Chemistry, Tel Aviv University, Ramat Aviv, 69978, Israel

Received 27 February 2007, in final form 11 March 2007
Published 13 August 2007
Online at stacks.iop.org/JPhysCM/19/375113

Abstract

Interfaces between two immiscible electrolytic solutions (ITIES), which are impermeable to ion transfer over a large potential range, offer immensely better opportunities for fine shape control at low voltages than current electrowetting systems. Also, ITIES can be described by a theoretical model with few free parameters. This paper reveals, in full detail, the intricacies of a theory that can be used to describe electrowetting equilibrium (previously discussed briefly in Monroe *et al* (2006 *Phys. Rev. Lett.* **97** 136102)). Families of curves are presented to show how the contact angle between an ITIES and an electrode varies with voltage, to gauge expectations for laboratory measurements. A detailed analysis of the system construction, usually absent in theoretical papers, is provided to illustrate how undesired artefacts due to experimental geometry can be avoided. To contrast the case of ITIES, an analysis is also given for systems with a completely ion-permeable liquid/liquid interface. Although the latter system is very difficult to engineer, its comparison to ITIES illustrates the unique features that the ion-impermeability of a liquid/liquid interface adds to its electrowetting response.

1. Introduction

When a liquid/liquid interface contacts a solid substrate, applied voltages can cause the interface to change shape. This *electrowetting* phenomenon affords an elementary means by which liquid/liquid interfaces can be functionalized. Devices reliant upon electrowetting require no internal machinery. Also, because shape is an equilibrium characteristic of a phase, interfaces in these devices self-assemble and are difficult to destabilize. Hence the growing popular ambition to exploit electrowetting in technologies like portable lenses, microfluidic devices and electronic displays [1–3].

Current electrowetting systems involve an insulating liquid, which forms an interface with an ionically conductive liquid [4]. Presumably this construction decreases the probability of irreversible Faradaic processes at the phase boundaries. However, it also complicates the system response significantly, because very high surface-charge densities can develop in the insulating fluid near the three-phase (liquid/liquid/substrate) contact line [5].

Recently the authors proposed a new class of electrowetting systems employing two ionically conductive fluids [6, 7]. In this configuration, Faradaic processes at the liquid/liquid interface can be prevented by using an Interface between Two Immiscible Electrolytic Solutions (ITIES). Research on ITIES goes back to the time of Nernst. Applications of ITIES mainly exploit adsorption characteristics, catalytic properties, mesoscale interfacial morphology and the energetics of ion solvation [8]. However, the macroscopic electrowetting properties of ITIES have gone relatively unnoticed.

ITIES-based systems have practical advantages for electrowetting applications. In current devices, applied potentials in the range of 10–100 V are needed to achieve significant shape variation [4]. With ITIES, similar shape changes can be induced with potentials of hundreds of millivolts. This difference arises because in typical systems the field distributes relatively evenly across the entire insulating-liquid phase, leading to significant voltage losses in its bulk, whereas with ITIES both solutions form double layers ('space-charge regions' of excess charge density very near phase boundaries) which localize potential drops over a distance of several nanometres from the interfaces. As well as reducing the voltages for shape change, this field localization makes the response of ITIES-based electrowetting systems relatively insensitive to electrode geometry.

In previous work our group developed the linear electrostatic response of ITIES-based systems consisting of an electrolytic droplet in contact with a metal electrode, both of which are surrounded by an ambient electrolytic solution. We showed that the three-phase contact line exhibits the divergent charge density characteristic of typical electrowetting systems, but that this divergence makes a negligible contribution to the free energy when droplets are sufficiently large [6].

Several groups have attributed contact-angle saturation (the approach to a limiting interfacial shape at high potentials) to field divergence near the three-phase contact line [4]. But in systems with ITIES, this effect does not influence the morphology of liquid/liquid interfaces, except for a region within nanometres of the contact line [6]. Thus the shapes of macroscopic ITIES are simpler to model than those of the liquid/liquid interfaces in typical electrowetting systems.

In a recent short communication [7], we extended our previous theory to describe the regime of large potentials. This work demonstrated that both contact-angle saturation and dewetting (the detachment of a liquid/liquid interface from its substrate) can be rationalized naturally by the conservation of material within the droplet, rather than field divergence.

This paper develops the theoretical basis of our previous work in substantially greater detail. Here we derive the free-energy functional used in [7], revealing a number of avenues by which simplifying assumptions can be relaxed. We also present a comprehensive set of calculated results for ITIES with a range of properties. In addition, we treat the case where there are two conductive fluids that contain a mutually miscible salt, which has not been considered before.

The detailed treatment of electrowetting equilibria given below also provides information which could guide the development of more precise computer simulations. The analysis shows how to obtain (and generalize) every differential equation that would have to be solved simultaneously in a numerical electrowetting model; it elucidates several physical constraints that apply to the distributions which satisfy these equations, such as the equation of state, the preservation of total ion content and the conservation of charge; it permits extension to nonideal solutions, the analysis of which may be tractable only by numerical methods; it shows how the experimental electrode geometry comes into play—and how the geometry of the counter and reference electrodes may be important; and, finally, it lays out an analytical procedure that could be paralleled step by step with an automated process.

This paper is organized as follows. Section 2 develops a general thermodynamic approach which is applicable to any equilibrated electrowetting system—including both conventional systems and those with ITIES. A simplified form of the free-energy functional is developed. Section 3 applies this simplified functional to find the equilibrium shape of an ITIES in contact with a metal working electrode. Additional consideration is given to the shapes and sizes of the reference and counterelectrodes, which are often neglected. Section 4 addresses electrowetting scenarios with two ionically conductive fluids and a fully ion-permeable interface, for comparison to ITIES.

The appendix provides a case study for the potential-dependent part of the functional. A tutorial example, the parallel-plate double-layer capacitor, is treated to show how ion-impermeable phase boundaries affect the distributions of ion concentration and potential within a moderately dilute electrolytic solution. This appendix substantiates and defines many of the physico-chemical principles applied in the main body of the work.

2. Thermodynamics of electrowetting

2.1. The free-energy functional

The equilibrium state of an electrowetting system at constant temperature and pressure is characterized by the Gibbs free energy of the system, G. Its three primary constituents are capillary energy, electrostatic energy, and electrochemical work:

$$G = \mathscr{C} + \mathscr{V} + \mathscr{W}. \tag{2.1}$$

Capillary energy, $\mathscr{C}$, depends on the surface tension and area of each two-phase interface in the system. Electrostatic energy, $\mathscr{V}$, is defined as the work withdrawn from the system by an external circuit connected to electrodes immersed in the system. $\mathscr{V}$ is negative when a voltage source inputs energy to maintain charges on the electrodes. The electrochemical work, $\mathscr{W}$, is formed by the sum of electrochemical potentials of all the molecular or ionic species in bulk phases between the electrodes. It includes local charge–charge interactions, mixing free energy, and short-range specific interactions within each phase, as well as the work done by external pressure on the phases.

A suitable approach to any equilibrium electrowetting problem is to express $\mathscr{C}$ and $\mathscr{V}$ in forms appropriate to the number of distinct phases, introduce constitutive laws for the species in each phase to write $\mathscr{W}$, and then minimize the variation in G with appropriate constraints to determine the interfacial shapes. This section considers the contributions to G in detail and introduces physical conditions to simplify the functional before its variation is taken.

Most electrowetting scenarios involve several phases which need to be considered during analysis: two types of fluid, the working electrode, the counterelectrode, and, possibly, a reference electrode (or electrodes) immersed in the fluids. Here we consider only systems with the geometry depicted schematically in figure 1. The figure shows a single liquid droplet (phase d) surrounded by an ambient fluid (phase s). Both of the fluids contact a working electrode (phase e), and the counterelectrode (phase c) touches the surrounding fluid only.

If ions are dissolved in the surrounding fluid, a single reference electrode (phase r), which is electrochemically reversible[3] to one of the ions, may also be placed in its bulk (far from e,

[3] Reference electrodes *must* undergo oxidation or reduction reactions with one of the ions dissolved in the surrounding electrolyte. Such a condition gives the 'potential drop' thermodynamic significance. Meaningful comparison of the electrochemical work in two systems with differing chemical composition is only possible when the potentials in both systems involve reversible reference electrodes and both potentials are referred to the same redox couple. A reference electrode allows the potentials at electrodes e and c to be varied independently, and permits the differing chemistry occurring at these interfaces to be assessed. Only a few sets of carefully referenced electrowetting data have been published; for an excellent set of experiments see [9].

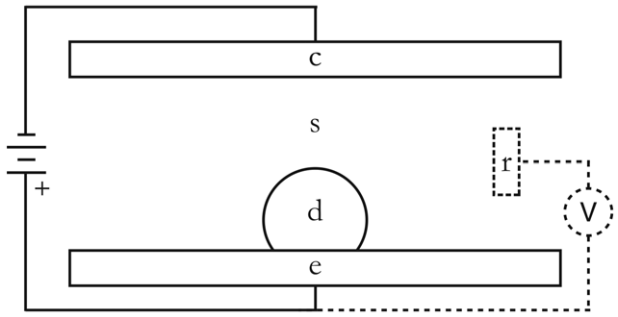

Figure 1. Diagram of the experimental geometry, with labels corresponding to the various phases.

c, and d). In this case a voltage source which applies a potential drop between e and c can be used to control the voltage read by the voltmeter, V.

2.2. Capillary term

The capillary energy in this system takes the form

$$\mathscr{C} = \gamma_{\mathrm{de}} A_{\mathrm{de}} + \gamma_{\mathrm{se}} A_{\mathrm{se}} + \gamma_{\mathrm{ds}} A_{\mathrm{ds}} + (\gamma_{\mathrm{sc}} A_{\mathrm{sc}} + \gamma_{\mathrm{sr}} A_{\mathrm{sr}}), \tag{2.2}$$

where γ_{jk} is the surface tension and A_{jk} the interfacial area between phases j and k. These surface tensions are defined in the absence of an external electric field and are therefore constant with respect to potential.

In equation (2.2) the terms involving the counter and reference electrodes are written in parentheses because they are often omitted. Their omission from $\mathscr{C}$ is justified only if the counter and reference electrodes have static shapes, if both remain in contact with a single fluid for any droplet shape, and if the counterelectrode is very large. Under these conditions the parenthetical term cancels further along in the analysis, when G is expressed relative to a droplet-free reference state. Otherwise the term should be borne in mind; it is considered in detail in section 3.2.

2.3. Electrostatic term

In practice $\mathscr{V}$ is supplied by a potentiostat, which maintains a fixed potential difference between the working electrode and either the counterelectrode or reference electrode. For the system in figure 1, the electrostatic work that can be produced by an electric field **E** which permeates the droplet and surrounding fluid is

$$\mathscr{V} = -\frac{\epsilon_0}{2} \sum_{j=\mathrm{d,s}} \int_{V_j} \epsilon_j \mathbf{E} \cdot \mathbf{E} \, \mathrm{d}V, \tag{2.3}$$

where ϵ_0 is the permittivity of free space and ϵ_j and V_j are the dielectric constant and volume of phase j, respectively. Because the field may not be uniform within the droplet and its surroundings, $\mathscr{V}$ is generally an integral over the two fluid phases. The specific properties of the working, counter and reference electrodes do not appear in this equation explicitly; they remain to be introduced later through boundary conditions on the electric field or potential.

2.4. Electrochemical term

In general $\mathscr{W}$ includes mechanical work, due to pressure differences between the droplet bulk and the bulk of its surroundings, mixing free energy, due to irregular distributions of molecules

within each phase, and Coulomb energy, due to the localization of discrete ionic charges in solution. For a given species i in phase j these effects can all be expressed through the pressure, temperature, voltage and composition dependence of the electrochemical potential, μ_{ji}.

In a three-phase system where each fluid phase contains I_j components, the electrochemical work is

$$\mathscr{W} = \sum_{j=\mathrm{d,s}} \sum_{i=1}^{I_j} \int_{V_j} c_{ji}\mu_{ji}\,\mathrm{d}V, \tag{2.4}$$

where c_{ji} is the molar concentration of species i in phase j. This expression is also written as an integral, because c_{ji} and μ_{ji} may vary locally within the droplet and surrounding fluid.

The constitutive law—Electrochemical potentials are given generally by [10]

$$\mu_{ji} = RT\ln(a_i^{\ominus} f_{ji} x_{ji}) + z_{ji}F\Phi, \tag{2.5}$$

in which R is the gas constant, T is the absolute temperature and F is Faraday's constant; $a_i^{\ominus}$ is the activity of species i in a secondary reference state (a state such as 'pure component i', at the same temperature and pressure as phase j: more details, and definitions of reference states for ions, are discussed in [10]). The particle fraction, equivalent charge and activity coefficient of species i in phase j are respectively denoted by x_{ji}, z_{ji} and f_{ji}. Here Φ is an electrostatic potential, related to the electric field by $\mathbf{E} = -\nabla\Phi$.

Two physical considerations restrict the degrees of freedom available to parameters in the constitutive law and must be obeyed for thermodynamic consistency. First, the particle fractions in each phase sum to unity, $\sum_i x_{ji} = 1$. Thus $(I_j - 1)$ particle fractions specify the composition of phase j; consequently $f_{ji} = f_{ji}(T, p, x_{j1}, \ldots, x_{j(I_j-1)})$, where p is the external pressure (p is positive when forces are compressive). Second, the Gibbs–Duhem equation [10] relates the f_{ji} when multiple species are present, and consequently $f_{jn} = f_{jn}(T, p, f_{j1}, \ldots, f_{j(I_j-1)})$. For non-piezoelectric phases f_{ji} does not depend on Φ.

An equation of state for the total molar concentration of phase j, $c_{j\mathrm{T}}$, is

$$\frac{1}{c_{j\mathrm{T}}} = \sum_{i=1}^{I_j} \overline{V}_{ji} x_{ji}. \tag{2.6}$$

The partial molar volume $\overline{V}_{ji}$ is defined as

$$\overline{V}_{ji} = \left(\frac{\partial V_j}{\partial n_{ji}}\right)_{T,p,n_{jk,k\neq i}} = \left(\frac{\partial \mu_{ji}}{\partial p}\right)_{T,n_{jk}}, \tag{2.7}$$

where the second identity is a Maxwell relation obtained from $\mathrm{d}G$. Thus the equation of state for phase j is contained in the constitutive laws for μ_{ji}.

Electrochemical potentials in ideal solutions—A simpler constitutive law applies in cases where the solutions behave ideally. An *ideal solution* is defined as one for which the partial molar volumes of all species are constant, independent of composition; also, for solute i, $f_{ji} = 1$. Then for all species, including the solvent,

$$\mu_{ji} = RT\ln x_{ji} + z_{ji}F\Phi + \overline{V}_{ji}p + \text{constant}. \tag{2.8}$$

In an isothermal system the constant can be discarded: it is independent of p, Φ and all x_{ji}. Insertion of equation (2.8) into $\mathscr{W}$ gives

$$\mathscr{W} = \sum_{j=\mathrm{d,s}} \left[RT \int_{V_j} c_{j\mathrm{T}} \sum_{i=1}^{I_j} x_{ji}\ln x_{ji}\,\mathrm{d}V + \int_{V_j} \rho_j\Phi\,\mathrm{d}V + \int_{V_j} p\,\mathrm{d}V \right], \tag{2.9}$$

where the shorthand notation ρ_j indicates the local excess charge density in solution j,

$$\rho_j = F \sum_{i=1}^{I_j} z_{ji} c_{ji}. \tag{2.10}$$

In equation (2.9), the first term in the brackets accounts for the free energy of mixing; the second, for the Coulombic interactions among dissolved charged species; and the third, for mechanical work.

Insertion of equations (2.2) (for $\mathscr{C}$), (2.3) (for $\mathscr{V}$), and (2.9) (for $\mathscr{W}$) into equation (2.1) (for G) gives a free-energy functional that describes single-droplet electrowetting equilibrium in a broad range of experimental circumstances.

Ideal versus nonideal—For moderately dilute solutions, the ideal-solution approximation is known to describe the space-charge distributions near interfaces fairly accurately. It will be used throughout the remainder of this work. However, this section has provided the structural framework needed to extend the description to nonideal solutions.

3. Electrowetting with ITIES

The variational approach to the electrostatic and electrochemical parts of the free-energy functional is relatively involved. A summary of the general principles applicable to electrolytic phases with impermeable boundaries is given in the appendix, where the variational procedure is illustrated by a simple example. Interested readers may want to consult the appendix at this point. It summarizes the qualitative principles applicable to any electrolytic phase which conserves its contents under potential bias. Also, a number of analytical details are provided there which justify the choice of electrostatic governing equations and constraints here.

This section treats the electrowetting geometry shown in figure 1 for a situation where the interface between phases d and s is an ITIES. The most significant physical feature of ITIES is that the ions in both solutions have very high free energies of transfer. One solution typically consists of a 'fatty' salt, such as tetrabutylammonium tetraphenylborate, dissolved in an organic solvent, like nitrobenzene. The other solution is usually composed of an alkali halide, such as lithium chloride, dissolved in water. Both salts are extremely well solvated in their phases of origin. The liquid/liquid interface behaves as if it is impermeable to ions from either side (i.e. it is ideally polarizable). Inspection of the capacitance response of ITIES shows that this behaviour can manifest over a broad potential range [11]. Thus in an electrowetting system with an ITIES, the droplet phase conserves its contents—no ions enter or leave it when a voltage within the ideal-polarizability window is applied. The conservation of droplet contents plays an important role in determining the electrostatic and shape equilibrium of the system.

It is assumed that no Faradaic processes occur at the working and counterelectrodes (i.e. they are also ideally polarizable). Therefore the surrounding phase also conserves its contents under potential bias.

The following subsections treat electrowetting of ideal, dilute ITIES, for which the free-energy functional was derived in section 2. Note that the electrostatic analysis relies on many of the basic procedures laid out in appendix A.2, which are avoided for brevity here.

Functional analysis of ITIES-based electrowetting is more intricate than the simpler example shown in the appendix, which involves only one liquid phase. In the case of ITIES, two liquids, with characteristic electrolytic properties, internal pressures and volumes must be considered. Also, for the experimental geometry shown in figure 1, interphase contact areas of five different types come into play.

Because the surrounding solution contains a buffer, it is appropriate to measure the potential drop relative to a reference electrode in the bulk of the surroundings (phase r in figure 1), rather than relative to the counterelectrode (phase c). Below, the working-to-reference potential drop is taken to be an experimentally controlled parameter.

3.1. The droplet-free reference state

When considering capillary and mechanical terms in the free-energy functional, the first concerns are the volumes of the droplet and the surroundings, V_d and V_s, and the areas of the five two-phase interfaces, A_se, A_de, A_ds, A_sc and A_sr (cf figure 1). Typically V_d is fixed experimentally by, say, placing the droplet on the surface of the working electrode with a micropipette. When capillary equilibrium is reached without an applied voltage, there is a repeatable correspondence between V_d and A_de.

If voltages are varied, all of the geometric parameters must be considered; the surface-charge densities at every one of the five interfaces may depend on their geometry. In different experimental setups, the areas A_se, A_sc and A_sr, and the volume of the surrounding fluid, V_s, may be of arbitrary size compared to the droplet. (And these sizes are typically not reported.) However, the description can still be reduced essentially to a correspondence between V_d and A_de if the system free energy is expressed as an excess function. It is therefore convenient to write G as a free-energy difference, relative to the free energy of a state with the same electrode geometry, with the same surrounding solution, at the same potential, but without a droplet. This reference scenario is called the *droplet-free state*.

To analyse the droplet-free state, consider the volume occluded by the droplet in figure 1 to instead be occupied by the surrounding solution. Then the entire space filled by the electrolyte, with *total* volume $V_\mathrm{T} = V_\mathrm{d} + V_\mathrm{s}$, has the properties of the surroundings. Similarly, the *total* area of the working electrode contacting the electrolyte, A_Te, is $A_\mathrm{Te} = A_\mathrm{de} + A_\mathrm{se}$.

As clarified in section A.2, if the surrounding phase is an isothermal, dilute, ideal electrolytic solution, then its ions are Boltzmann distributed with respect to potential. The electrostatic and internal-work contributions to G can therefore be re-expressed in terms of two simpler functionals, one dependent on Φ only, and one dependent only on the pressure distribution:

$$\mathscr{V}[\Phi] + \mathscr{W}[c_{\mathrm{s}+}, c_{\mathrm{s}-}, \Phi, p_\mathrm{s}] = \mathscr{E}[\Phi] + \int_{V_\mathrm{T}} p_\mathrm{s}\,\mathrm{d}V. \tag{3.1}$$

For electrolytic solutions with 1:1 salt stoichiometry in the droplet-free state, $\mathscr{E}$ is given by

$$\mathscr{E} = -RTc_\mathrm{s}^\mathrm{ref}\left[\frac{1}{\kappa_\mathrm{s}^2}\int_{V_\mathrm{T}} \nabla\phi\cdot\nabla\phi\,\mathrm{d}V + 2\int_{V_\mathrm{T}} [\cosh(\phi-\phi_\mathrm{s}^\mathrm{ref}) - 1]\,\mathrm{d}V\right], \tag{3.2}$$

where dimensionless potentials ϕ and $\phi_\mathrm{s}^\mathrm{ref}$ are defined as

$$\phi = \frac{zF\Phi}{RT} \qquad \text{and} \qquad \phi_\mathrm{s}^\mathrm{ref} = \frac{zF\Phi_\mathrm{s}^\mathrm{ref}}{RT} \tag{3.3}$$

to simplify notation. (At room temperature, these represent potentials counted in units of ~ 25 mV.) Other dimensionless potentials are used later and have analogous definitions. The inverse Debye length, κ_s, is

$$\kappa_\mathrm{s} = \sqrt{\frac{2F^2z^2\langle c_\mathrm{s}\rangle}{\epsilon_0\epsilon_\mathrm{s}RT}}, \tag{3.4}$$

where $\langle c_\mathrm{s}\rangle$ is the average salt concentration in the surroundings. Because the salt is 1:1, $z_{\mathrm{s}+} = -z_{\mathrm{s}-} = z$.

In equation (3.2), both ϕ_s^{ref} and c_s^{ref} are Lagrangian parameters, which satisfy constraints on the potential and concentration distributions. Impermeability of the boundaries of V_T requires that self-consistent results satisfy two conditions: (1) the interior of the region must have zero total charge and (2) the total amount of salt within the region must be the same at all applied potentials. These constraints can both be expressed as integrals of the ion-concentration distributions, and used to determine the bulk potential ϕ_s^{ref} and the reference concentration c_s^{ref}.

The reference concentration can be thought of as the 'bulk salt concentration', which in general is slightly lower than $\langle c_s \rangle$ because applied voltages draw ions toward both electrodes. (Appendix A.2 justifies this statement in greater detail.) By placing a lower bound on the phase size, c_s^{ref} can be eliminated, as implemented shortly.

The variation of $\mathscr{E}$ with respect to potential shows that ϕ obeys a nonlinear Poisson–Boltzmann equation similar to equation (A.11):

$$\frac{1}{(\chi_s \kappa_s)^2} \nabla^2 (\phi - \phi_s^{ref}) = \sinh(\phi - \phi_s^{ref}). \tag{3.5}$$

Here χ_s is the inverse-Debye-length reduction factor, determined by differences between the bulk concentration and the average concentration: $\chi_s = \sqrt{c_s^{ref}/\langle c_s \rangle}$.

Equation (3.5) should be solved subject to boundary conditions where $\phi_s = \phi_e$ at the surface of working electrode e, $\phi_r = \phi_s^{ref}$ at the surface of reference electrode r (because the electrochemical reaction at its surface is in equilibrium with phase s) and $\phi_s = \phi_c$ at the surface of the counterelectrode.

The potential difference $\Delta\phi = (\phi_e - \phi_r) = (\phi_e - \phi_s^{ref})$ is experimentally controlled. As shown below, the working-to-counter potential difference $(\phi_e - \phi_c)$ can be related to $\Delta\phi$ because V_T has ion-impermeable boundaries.

Several principles summarized in appendix A.4 now come in handy. First, if the distance between electrodes is greater than ~1000 Debye lengths, then c_s^{ref} in equation (3.2) can be safely taken to equal the average concentration (cf equation (A.21)); consequently $\chi_s = 1$ in equation (3.5). This also allows concentration overpotentials induced by $\Delta\phi$ to be neglected at the surface of the reference electrode. Second, if the average interelectrode distances are more than a few hundred Debye lengths, then the potential distribution in the solution as a function of the distance y normal to the surface of electrode e is

$$\phi_{se}(y) = 2 \ln \left[\frac{1 + \tanh\left(\frac{1}{4}\Delta\phi\right) e^{-\kappa_s y}}{1 - \tanh\left(\frac{1}{4}\Delta\phi\right) e^{-\kappa_s y}} \right] + \phi_s^{ref}. \tag{3.6}$$

This is the familiar nonlinear Gouy–Chapman result [12, 13], modified such that the potential reaches ϕ_s^{ref} in the bulk and the potential drop $\Delta\phi = \phi_e - \phi_s^{ref}$ is fixed.

In principle, if the working and counterelectrode are far apart, they need not be parallel. At a distance y' normal to the surface of counterelectrode c, the potential distribution in the solution is

$$\phi_{sc}(y') = 2 \ln \left[\frac{1 + \tanh\left[\frac{1}{4}\Delta\phi - \frac{1}{4}(\phi_e - \phi_c)\right] e^{-\kappa_s y'}}{1 - \tanh\left[\frac{1}{4}\Delta\phi - \frac{1}{4}(\phi_e - \phi_c)\right] e^{-\kappa_s y'}} \right] + \phi_s^{ref}. \tag{3.7}$$

From these it follows that the surface-charge densities at electrodes e and c are

$$\sigma_e = -2\epsilon_0 \epsilon_s \kappa_s \sinh(\tfrac{1}{2}\Delta\phi) \qquad \text{and} \qquad \sigma_c = -2\epsilon_0 \epsilon_s \kappa_s \sinh[\tfrac{1}{2}\Delta\phi - \tfrac{1}{2}(\phi_e - \phi_c)]. \tag{3.8}$$

But, because the electrolytic solution has ion-impermeable boundaries, the total charge within it must be zero. Therefore the total surface charges at e and c are equal and opposite:

$$\sigma_e A_{Te} + \sigma_c A_{sc} = 0. \tag{3.9}$$

Thus

$$\Delta\phi = 2\tanh^{-1}\left[\frac{\sinh\left(\frac{1}{2}\phi_e - \frac{1}{2}\phi_c\right)}{\frac{A_{Te}}{A_{sc}} + \cosh\left(\frac{1}{2}\phi_e - \frac{1}{2}\phi_c\right)}\right] \tag{3.10}$$

gives the promised equation for $(\phi_e - \phi_c)$ in terms of $\Delta\phi$. Note that when $A_{Te}/A_{sc} \ll 1$, the potential drop reduces to $\Delta\phi = \phi_e - \phi_c$.

The same considerations used for the potential distributions can be applied to justify the expression of $\mathscr{E}$ per unit electrode area. When the interelectrode distance is very large compared to the Debye length ($>1000/\kappa$), the integral in equation (3.2) can be broken into two terms, each of which is a semi-infinite integral near one of the electrodes. Insertion of the potential distributions from equations (3.6) and (3.7) into the integral in equation (3.2) yields

$$\begin{aligned}\mathscr{E} &= -\frac{16RTc_s}{\kappa_s}\sinh^2\left(\tfrac{1}{4}\Delta\phi\right)A_{Te} - \frac{16RTc_s}{\kappa_s}\sinh^2\left[\tfrac{1}{4}\Delta\phi - \tfrac{1}{4}(\phi_e - \phi_c)\right]A_{sc} \\ &= \overline{\mathscr{E}}_{se}A_{Te} + \overline{\mathscr{E}}_{sc}A_{sc},\end{aligned} \tag{3.11}$$

where the last equality introduces the convenient notation $\overline{\mathscr{E}}_{ij}$ to indicate the potential-dependent energy per unit area at interface ij. Note that the overbar in $\overline{\mathscr{E}}_{ij}$ does not indicate an average: because the electrodes are equipotential surfaces, the volume integral is uniform in directions tangential to the interfaces.

All quantities related to the droplet-free state will henceforth be indicated with a superscript 0. For instance, the free energy of the droplet-free state is G^0. Incorporation of $\mathscr{C}$ from equation (2.2) into the general functional, equation (2.1), yields

$$G^0 = (\gamma_{se} + \overline{\mathscr{E}}^0_{se})A_{Te} + (\gamma_{sc} + \overline{\mathscr{E}}^0_{sc})A_{sc} + \gamma_{sr}A_{sr} + \int_{V_T} p_s^0\,\mathrm{d}V. \tag{3.12}$$

Here the two $\overline{\mathscr{E}}^0_{ij}$ are defined by equation (3.11), and the potential difference $(\phi_e - \phi_c)$, upon which $\overline{\mathscr{E}}^0_{sc}$ depends, is given implicitly in terms of $\Delta\phi$ by equation (3.10).

Note that the effective surface tension measured in electrochemistry is typically taken to depend on potential. In the present approach, γ_{ij} is taken to be constant (equal to the surface tension with no applied potential). The potential-dependent part of the surface energy is considered explicitly in $\mathscr{W}$ (cf equation (2.4)).[4]

3.2. *Electrostatics with ITIES*

Having established the background, droplet-free state, the electrowetting of an ITIES for the configuration shown in figure 1 can now be analysed. The analysis is limited to droplets with an average radius of curvature greater than 1000 droplet-phase Debye lengths. For droplets of this size, the energetic contribution of the three-phase contact line can be neglected [6]. The free-energy functional then reduces to

$$\begin{aligned}G = &\left(\gamma_{de} + \overline{\mathscr{E}}_{de}\right)A_{de} + \left(\gamma_{se} + \overline{\mathscr{E}}_{se}\right)A_{se} + \left(\gamma_{ds} + \overline{\mathscr{E}}_{ds}\right)A_{ds} + \left(\gamma_{sc} + \overline{\mathscr{E}}_{sc}\right)A_{sc} \\ &+ \gamma_{sr}A_{sr} + \sum_{j=d,s}\int_{V_j} p_j\,\mathrm{d}V.\end{aligned} \tag{3.13}$$

[4] Thus equation (3.12) can be used to derive a standard Lippmann equation [27], showing that the present approach is consistent with Gibbs–Lippmann theory. But the functional method specifies what constraints on phase volume are necessary for a Lippmann equation to be valid: if the electrolytic phase has a characteristic size much less than 1000 Debye lengths, then the volume integrals in equation (3.2) cannot be decomposed into independent surface contributions, and the Gibbs–Lippmann isotherm may fail.

This equation distinguishes several new potential-dependent energies per unit area: one at the electrode/surroundings interface, $\overline{\mathscr{E}}_{\mathrm{se}}$, one at the droplet/electrode interface, $\overline{\mathscr{E}}_{\mathrm{de}}$, and one at the droplet/surroundings interface, $\overline{\mathscr{E}}_{\mathrm{ds}}$. These are calculated below.

Because interface ds is an ITIES, the droplet boundaries are ion-impermeable. Therefore the droplet interior should be treated according to the procedure given in section A.2. There is a bulk potential within the droplet, $\phi_{\mathrm{d}}^{\mathrm{ref}}$, around which a potential plateau forms, as well as a bulk potential in the surroundings, $\phi_{\mathrm{s}}^{\mathrm{ref}}$. The droplet/surroundings interface is essentially an equipotential surface [6]. In the same way as in the droplet-free state, the potential difference $\Delta\phi = (\phi_{\mathrm{e}} - \phi_{\mathrm{r}}) = (\phi_{\mathrm{e}} - \phi_{\mathrm{s}}^{\mathrm{ref}})$ is experimentally controlled. (This definition requires that the reference electrode contacts the surrounding solution only.) The droplet is also taken to contain a 1:1 electrolyte.

Following the analytical procedure developed for the droplet-free state, one obtains

$$\overline{\mathscr{E}}_{\mathrm{se}} = -\frac{16RTc_{\mathrm{s}}}{\kappa_{\mathrm{s}}}\sinh^2\left(\tfrac{1}{4}\Delta\phi\right) \qquad \text{and} \qquad \overline{\mathscr{E}}_{\mathrm{de}} = -\frac{16RTc_{\mathrm{d}}}{\kappa_{\mathrm{d}}}\sinh^2\left(\tfrac{1}{4}\Delta\phi - \tfrac{1}{4}\phi_*\right), \tag{3.14}$$

where the latter introduces $\phi_* = (\phi_{\mathrm{d}}^{\mathrm{ref}} - \phi_{\mathrm{r}}) = (\phi_{\mathrm{d}}^{\mathrm{ref}} - \phi_{\mathrm{s}}^{\mathrm{ref}})$ to represent the potential of the droplet bulk relative to the reference electrode. Here κ_{d} has a definition analogous to κ_{s}, with the same value of z but with $\langle c_{\mathrm{s}}\rangle$ and ϵ_{s} replaced with $\langle c_{\mathrm{d}}\rangle$ and ϵ_{d}, respectively (see equation (3.4)). The surface-charge densities at the working electrode along contact areas se and de are

$$\sigma_{\mathrm{se}} = -\frac{2RT\epsilon_0\epsilon_{\mathrm{s}}\kappa_{\mathrm{s}}\sinh\left(\frac{1}{2}\Delta\phi\right)}{Fz} \qquad \text{and} \qquad \sigma_{\mathrm{de}} = -\frac{2RT\epsilon_0\epsilon_{\mathrm{d}}\kappa_{\mathrm{d}}\sinh\left(\frac{1}{2}\Delta\phi - \frac{1}{2}\phi_*\right)}{Fz}. \tag{3.15}$$

The energy and surface-charge density at the counterelectrode are

$$\begin{aligned} \overline{\mathscr{E}}_{\mathrm{sc}} &= -\frac{16RTc_{\mathrm{s}}}{\kappa_{\mathrm{s}}}\sinh^2\left[\tfrac{1}{4}\Delta\phi - \tfrac{1}{4}\left(\phi_{\mathrm{e}} - \phi_{\mathrm{c}}\right)\right] \qquad \text{and} \\ \sigma_{\mathrm{sc}} &= -\frac{2RT\epsilon_0\epsilon_{\mathrm{s}}\kappa_{\mathrm{s}}\sinh\left[\frac{1}{2}\Delta\phi - \frac{1}{2}\left(\phi_{\mathrm{e}} - \phi_{\mathrm{c}}\right)\right]}{Fz} \end{aligned} \tag{3.16}$$

These equations imply that the counterelectrode contacts only the surrounding solution.

The final portion of the electrostatic analysis involves the potential distribution at the liquid/liquid interface. Equations that describe this interface involve the Debye lengths and dielectric constants in both the droplet and the surrounding solution. Notation can be simplified significantly by introduction of the parameter C, defined as

$$C = \sqrt{\frac{\epsilon_{\mathrm{s}}\kappa_{\mathrm{s}}}{\epsilon_{\mathrm{d}}\kappa_{\mathrm{d}}}}. \tag{3.17}$$

The specific double-layer capacitance (per unit area) yielded by linear Gouy–Chapman theory [12, 13] is $\epsilon_0\epsilon\kappa$. Thus C^2 is the linear Gouy–Chapman capacitance of the surroundings over the linear Gouy–Chapman capacitance of the droplet.

For ITIES where the free energies of transfer for all ions are high, the potential distribution can be taken from the Verwey–Niessen theory [14]. This theory works fairly well, even in cases where free energies of transfer are only of order 0.1 eV [11, 15]. It shows that the potential-dependent contribution to the energy per unit area of interface ds is

$$\overline{\mathscr{E}}_{\mathrm{ds}} = \epsilon_0\sqrt{\epsilon_{\mathrm{d}}\epsilon_{\mathrm{s}}\kappa_{\mathrm{d}}\kappa_{\mathrm{s}}}\left(\frac{2RT}{Fz}\right)^2\left[\left(C + \tfrac{1}{C}\right) - \sqrt{\left(C + \tfrac{1}{C}\right)^2 + 4\sinh^2\left(\tfrac{1}{4}\phi_*\right)}\right]. \tag{3.18}$$

Also, on the droplet side of interface ds, the surface-charge density is

$$\sigma_{ds} = \frac{2RT\epsilon_0\sqrt{\epsilon_d\epsilon_s\kappa_d\kappa_s}\sinh\left(\frac{1}{2}\phi_*\right)}{Fz\left[\left(C+\frac{1}{C}\right)^2+4\sinh^2\left(\frac{1}{4}\phi_*\right)\right]^{1/2}}. \tag{3.19}$$

On the surroundings side of ds, the surface-charge density is equal and opposite to this.

Using σ_{de} and σ_{ds} from equations (3.15) and (3.19), one can determine ϕ_* in terms of $\Delta\phi$. The droplet interior has zero total charge, which can be expressed as a constraint on the surface charges at its boundaries:

$$\sigma_{de}A_{de} + \sigma_{ds}A_{ds} = 0. \tag{3.20}$$

Insertion of equations (3.15) and (3.19) and some algebraic rearrangement give

$$\frac{A_{de}}{A_{ds}} = \frac{C\sinh\left(\frac{1}{2}\phi_*\right)/\sinh\left(\frac{1}{2}\Delta\phi - \frac{1}{2}\phi_*\right)}{\sqrt{\left(C+\frac{1}{C}\right)^2+4\sinh^2\left(\frac{1}{4}\phi_*\right)}}. \tag{3.21}$$

Thus ϕ_* and $\Delta\phi$ relate to the interfacial areas which bound the droplet.

The surrounding-solution phase also sustains no total charge, allowing $(\phi_e - \phi_c)$ to be found in terms of $\Delta\phi$ and ϕ_*. The constraint on the surface charge of the surrounding solution is

$$-\sigma_{ds}A_{ds} + \sigma_{se}A_{se} + \sigma_{sc}A_{sc} = 0. \tag{3.22}$$

A negative sign appears because the surroundings side of ds has a surface-charge density opposite to that on the droplet side.

Insertion of equation (3.20) to replace $\sigma_{ds}A_{ds}$ with $-\sigma_{de}A_{de}$ (which has a simpler form), followed by insertion of the relevant surface-charge densities and manipulation with the total working-electrode area $A_{Te} = A_{de} + A_{se}$, gives a relationship between $\Delta\phi$, $(\phi_e - \phi_c)$ and ϕ_*:

$$\Delta\phi = 2\tanh^{-1}\left[\frac{\sinh\left[\frac{1}{2}(\phi_e-\phi_c)\right] + C^{-2}\sinh\left(\frac{1}{2}\phi_*\right)\frac{A_{de}}{A_{sc}}}{\frac{A_{Te}}{A_{sc}} + \cosh\left[\frac{1}{2}(\phi_e-\phi_c)\right] + \frac{A_{de}}{A_{sc}}\left[C^{-2}\cosh\left(\frac{1}{2}\phi_*\right)-1\right]}\right]. \tag{3.23}$$

Note that this equation reduces to equation (3.10) only when A_{de}/A_{sc} is very small, or in the stricter case where the whole working electrode is much smaller than the counterelectrode, $A_{Te}/A_{sc} \ll 1$. Thus, if it is not sufficiently large, the counterelectrode may play a role in determining the droplet shape, as elaborated in section 3.3.

Equations (3.14), (3.16) and (3.18) give the energies stored per unit area at each of the relevant phase boundaries in terms of $\Delta\phi$ (the working-to-reference potential drop), ϕ_* (the droplet-bulk-to-reference potential drop) and $(\phi_e - \phi_c)$ (the working-to-counter potential drop). Equations (3.21) and (3.23) supply two relations which can be used to obtain ϕ_* and $(\phi_e - \phi_c)$ self-consistently in terms of $\Delta\phi$ and geometric parameters. Thus, with $\Delta\phi$ fixed, the electrostatic problem is solved for droplets of arbitrary shape. All that remains is to find the droplet shape which minimizes the excess free energy.

3.3. Droplet shapes with ITIES

The free-energy functional relative to a droplet-free state, $\Delta G = G - G^0$, is

$$\Delta G = (\gamma_{de} - \gamma_{se} + \overline{\mathscr{E}}_{de} - \overline{\mathscr{E}}^0_{se})A_{de} + (\gamma_{ds} + \overline{\mathscr{E}}_{ds})A_{ds} + (\overline{\mathscr{E}}_{sc} - \overline{\mathscr{E}}^0_{sc})A_{sc} + \int_{V_d}(p_d - p_s^0)\,dV. \tag{3.24}$$

The arbitrarily large area A_{se} and the portion of the volume integral that ranges over V_s cancel upon subtraction. Cancellation is possible because $\overline{\mathscr{E}}_{se} = \overline{\mathscr{E}}^0_{se}$ and, in V_s, $p_s = p_s^0$.

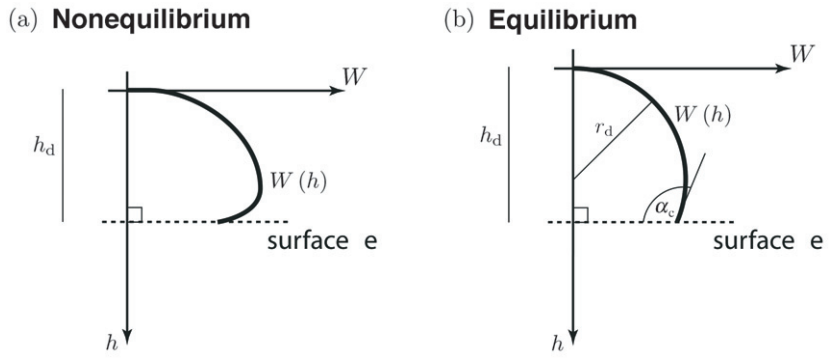

Figure 2. Schematic diagram of axes used for Euler–Lagrange analysis of droplet shapes. Rotational symmetry is assumed about the h-axis. The height of the droplet apex is h_d. (a) An arbitrary member of the family of functions $W(h)$. (b) The equilibrium surface profile which satisfies equation (3.28)—the surface has constant radius of curvature r_d and a surface contact angle α_c.

This functional simplifies further by adopting two additional approximations. First, the area of contact between the counterelectrode and the surroundings, A_{sc}, is taken to be large compared to the droplet/electrode contact area A_{de}. In that case a comparison of equations (3.10) and (3.23) shows that the working-to-counter potential drop ($\phi_e - \phi_c$) in the droplet-free state is the same as in the state with the droplet: $\overline{\mathscr{E}}_{sc} = \overline{\mathscr{E}}^0_{sc}$. Second, if the droplet is sufficiently small that the buoyant force on it due to gravity can be neglected, then the pressure distributions can be replaced with constants. The functional becomes

$$\Delta G = (\gamma_{de} - \gamma_{se} + \overline{\mathscr{E}}_{de} - \overline{\mathscr{E}}^0_{se})A_{de} + (\gamma_{ds} + \overline{\mathscr{E}}_{ds})A_{ds} + V_d \Delta p, \tag{3.25}$$

where Δp is the difference between the external pressure in the droplet bulk and the ambient pressure[5]. This pressure difference is a Lagrangian parameter, the value of which is set by the constraint that V_d is constant.

To find the droplet shape: consider an axis h which extends from the droplet apex (where $h = 0$) toward the working electrode, intersecting de normally to its surface (at $h = h_d$). Thus the height of the droplet apex is h_d and the shape of the liquid/liquid interface is a member of the family of functions $W(h)$. A schematic diagram is shown in figure 2.

The relevant interfacial areas are given in terms of W by

$$A_{de} = \pi W^2(h_d) \qquad \text{and} \qquad A_{ds} = 2\pi \int_0^{h_d} W(h)\sqrt{1 + \left(\frac{dW}{dh}\right)^2}\, dh, \tag{3.26}$$

and the droplet volume is

$$V_d = \pi \int_0^{h_d} W^2(h)\, dh. \tag{3.27}$$

After these are put into equation (3.25), the corresponding Euler–Lagrange equation reads

$$\frac{W''}{\left[1 + (W')^2\right]^{3/2}} - \frac{1}{W\left[1 + (W')^2\right]^{1/2}} = \frac{\Delta p}{\gamma_{ds} + \overline{\mathscr{E}}_{ds}}. \tag{3.28}$$

[5] When all the $\overline{\mathscr{E}}_{ij}$ are taken to be zero (that is, when $\Delta\phi = 0$, or if electrochemical energy $\mathscr{E}$ is neglected), this expression becomes the functional from which the Young–Laplace equation is usually derived [16].

This is a differential equation for $W(h)$; the right side depends on system parameters but is constant with h.

If $W(h)$ describes a circular arc with constant radius of curvature r_d, and $W'(0) = \infty$, as required by axial symmetry about the droplet apex, then

$$W(h) = \sqrt{r_d^2 - (r_d - h)^2} = \sqrt{h(2r_d - h)}, \tag{3.29}$$

and the geometric parameters become

$$A_{de} = \pi h_d(2r_d - h_d), \qquad A_{ds} = 2\pi h_d r_d, \qquad \text{and} \qquad V_d = \pi h_d^2(r_d - \tfrac{1}{3}h_d). \tag{3.30}$$

Then the Euler–Lagrange equation reduces to

$$\Delta p = -\frac{2(\gamma_{ds} + \overline{\mathscr{E}}_{ds})}{r_d}, \tag{3.31}$$

independent of h. It has been proved that equation (3.29) represents a *unique* solution to the augmented Euler–Lagrange formula in equation (3.28) [6]. Thus, even with applied potentials, the free energy is minimal when the droplet is a plane-truncated sphere[6]. Because r_d is constant, equation (3.31) also allows the Lagrangian parameter Δp to be exchanged for r_d.

Insertion of equations (3.30) and (3.31) into (3.25) gives

$$\Delta G = \pi(\gamma_{de} - \gamma_{se} + \overline{\mathscr{E}}_{de} - \overline{\mathscr{E}}^0_{se})h_d(2r_d - h_d) + 2\pi(\gamma_{ds} + \overline{\mathscr{E}}_{ds})h_d\left(r_d - h_d + \frac{h_d^2}{3r_d}\right), \tag{3.32}$$

which can be optimized with respect to the height of the droplet apex, h_d. Set $\partial\Delta G/\partial h_d = 0$ and rearrange to show

$$1 - \frac{h_d}{r_d} = \frac{(\gamma_{se} + \overline{\mathscr{E}}^0_{se}) - (\gamma_{de} + \overline{\mathscr{E}}_{de})}{\gamma_{ds} + \overline{\mathscr{E}}_{ds}}. \tag{3.33}$$

After all this, it is finally permitted to apply the constraint on droplet volume. This relates the radius of a plane-truncated sphere to its apex height through

$$r_d = \frac{V_d}{\pi h_d^2} + \frac{h_d}{3}. \tag{3.34}$$

Substitution of equation (3.34) into (3.33) gives a cubic equation for the apex height which minimizes ΔG at a given $\Delta\phi$.

3.4. Contact angles for electrowetting with ITIES

Governing equations for equilibrium contact angles—During experimental measurements, the height of the droplet apex alone is not important. Typically one measures the contact angle at the three-phase contact line. Let α_c denote the internal contact angle of the droplet with the working electrode. Then

$$\cos\alpha_c = 1 - \frac{h_d}{r_d} \qquad \text{and} \qquad \frac{A_{de}}{A_{ds}} = A = \frac{1 + \cos\alpha_c}{2}. \tag{3.35}$$

The first relation shows that equation (3.33) gives the cosine of the contact angle explicitly. Note that the second introduces the notation $A = A_{de}/A_{ds}$.

[6] Although [6] proved uniqueness in the linear potential regime, it is straightforward to extend the method shown there to the nonlinear case. Note that the droplet will not be a truncated sphere in cases where the solid substrate is not an equipotential surface or if buoyant forces are significant. The former is not the case for metal electrodes, and the latter can be neglected if the droplet mass is very small, or if the density difference between the fluids is negligible.

Two cumulative dimensionless parameters simplify the final expressions. The first, b, characterizes the relative importance of electrostatic and capillary forces:

$$b = \frac{\epsilon_0\sqrt{\epsilon_d\epsilon_s\kappa_d\kappa_s}}{\gamma_{ds}}\left(\frac{RT}{Fz}\right)^2. \tag{3.36}$$

The second, $\cos\alpha_c^0$, is the droplet/electrode contact angle without an applied potential:

$$\cos\alpha_c^0 = \frac{\gamma_{se} - \gamma_{de}}{\gamma_{ds}}, \tag{3.37}$$

which is simply Young's equation from the capillary theory.

Incorporation of the quantities A, b and $\cos\alpha_c^0$ allows the result for the contact-angle variation of an ideal, dilute ITIES to be written as

$$\cos\alpha_c = 2A\,(\Delta\phi, \phi_*) - 1, \tag{3.38}$$

where

$$A\,(\Delta\phi, \phi_*) = \frac{C\sinh\left(\frac{1}{2}\phi_*\right)/\sinh\left(\frac{1}{2}\Delta\phi - \frac{1}{2}\phi_*\right)}{\sqrt{\left(C + \frac{1}{C}\right)^2 + 4\sinh^2\left(\frac{1}{4}\phi_*\right)}}, \tag{3.39}$$

and ϕ_* is obtained from the transcendental equation

$$8b\left[\tfrac{1}{C}\sinh^2\left(\tfrac{1}{4}\Delta\phi - \tfrac{1}{4}\phi_*\right) - C\sinh^2\left(\tfrac{1}{4}\Delta\phi\right)\right] + \cos\alpha_c^0 + 1 - 2A(\Delta\phi, \phi_*) + 4b\left[\left(C + \tfrac{1}{C}\right) - \sqrt{\left(C + \tfrac{1}{C}\right)^2 + 4\sinh^2\left(\tfrac{1}{4}\phi_*\right)}\right][1 - 2A(\Delta\phi, \phi_*)] = 0. \tag{3.40}$$

The first relation follows from the definition of A; the second comes from the charge constraint on the droplet interior, through equations (3.21) and (3.35). The last equation determines ϕ_*, and was obtained by insertion of equations (3.14) and (3.18) into (3.33). As stated before, the working-to-reference potential drop $\Delta\phi$ is subject to experimental control by a potentiostat. The parameters C and b are fixed by the choice of solution composition in both phases, and $\cos\alpha_c^0$ additionally depends on the electrode material (cf equations (3.17), (3.36) and (3.37)).

Summary of approximations—It is worthwhile to summarize the approximations made to find equations (3.38)–(3.40):

(1) The working electrode and counterelectrode were assumed to be ideally polarizable. If significant Faradaic processes occur in a system, a dynamic theory is required.
(2) The droplet and surrounding liquid were taken to be ideal, dilute electrolytic solutions, which restricts the results to moderate or low salt concentrations in both liquids. This could be relaxed by adopting the more general law for bulk electrochemical potentials given in section 2.4.
(3) It was assumed that the area of contact between the counterelectrode and the surroundings is much larger than the droplet/electrode contact area. If necessary this approximation could be relaxed by retaining the full equation (3.23).
(4) Specific adsorption of ions at the electrodes was neglected. This could be relaxed by incorporating additional planar phases near the electrodes, in adsorption equilibrium with the bulk, using appropriate isotherms (Langmuir, Frumkin, etc).
(5) Diffuse Gouy–Chapman theory was adopted near the electrode surfaces. With large applied potentials, the so-called 'compact-layer' contribution, neglected above, may become significant [17, 18]. This effect will be considered elsewhere.

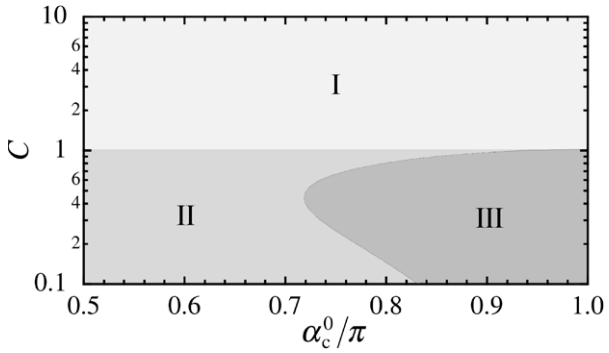

Figure 3. Characteristic responses of α_c to rising $\Delta\phi$ for electrowetting with an ITIES, plotted as a phase diagram in the C/α_c^0 plane, with $b = 0.005$. (I) Angle rises until dewetting. (II) Angle rises until saturation. (III) Angle initially falls, but reverses, with eventual saturation. (Figure reprinted from [7].)

(6) The previous two assumptions relate to the 'potential of zero charge' (PZC), which is an important concept in electrochemistry. In particular, the diffuse-layer capacitance has a minimum at the PZC. We have assumed for simplicity that the PZC for both solutions are equal, and coincide with the open-circuit potential measured relative to the reference electrode. The PZC between the two electrode/electrolyte interfaces can be included, but this introduces two unknown parameters to the problem. Measurement of these parameters is a challenging electrochemical problem in itself; once such data are available, they can be incorporated into the boundary conditions when solving the electrostatic governing equations.
(7) The interelectrode distances and the droplet radius were taken to be greater than 1000 Debye lengths ($\sim$1 μm at typical concentrations), placing a lower limit on system size.
(8) An upper limit on droplet size (or, alternatively, a constraint on the solution densities) was imposed by the neglect of buoyant forces.

Some of these approximations were made solely to achieve compact results. They can all be relaxed, but at the cost of analytical transparency. Numerical solution of the appropriate electrostatic governing equations, by finite-element procedures or otherwise, followed by numerical solution of the resulting Euler–Lagrange equation for shape, would be the methods of choice for computer simulations.

Results and discussion—Contact-angle responses of ITIES were described briefly in [7]. A more complete picture is provided here.

The contact-angle response falls into three regimes, determined mainly by C and $\cos\alpha_c^0$. A phase diagram for contact-angle response yielded by equations (3.38)–(3.40) is given in figure 3. Key features shown on the diagram are:

(1) Due to the constraint on its interior charge, the droplet's contact angle begins to rise when $\Delta\phi$ becomes sufficiently large. That is, the droplet/electrode contact area will eventually contract, no matter what the composition of the surrounding phase.
(2) When $C > 1$, the potential drop may cause the droplet to leave the electrode surface altogether (dewetting). When $C < 1$, it is not favourable for the droplet to leave the surface. Instead, the contact angle saturates to a limiting angle as the potential rises.
(3) When $C < 1$ and the initial contact angle is obtuse the contact angle may decrease, i.e. the droplet/electrode contact area may expand, at low or moderate potentials.

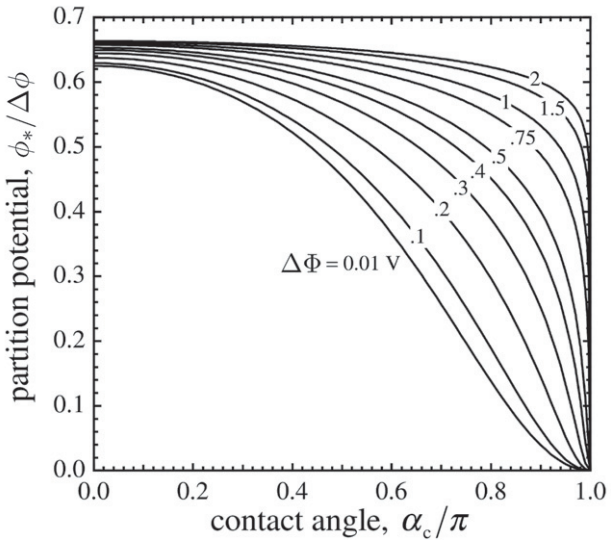

Figure 4. The partition factor $\phi_*/\Delta\phi$ as a function of α_c for $C = 1.225$. Contours show that partitioning of potential to the droplet bulk increases with the dimensional potential drop $\Delta\Phi$. At equilibrium, both ϕ_* and α_c must satisfy all three of equations (3.38)–(3.40) for a given $\Delta\Phi$. This figure shows the formal relationship among ϕ_*, α_c, and $\Delta\Phi$ determined by equations (3.38) and (3.39) alone, which depends on the capacitance ratio C only. For a particular system, equilibrium corresponds to a single point on each equipotential contour, the position of which also satisfies equation (3.40) and depends on b and α_c^0.

In previous work [7] the properties of ϕ_* were not addressed. However, since ϕ_* is a signature of the charge conservation within the droplet, its behaviour helps to illuminate how the system functions. The partition factor, $\phi_*/\Delta\phi$, gives the fraction of the applied working-to-reference potential drop that occurs across the liquid/liquid interface. Potential partitioning may be important for phase-transfer catalysis applications, in which it can affect reaction kinetics.

The partition factor can be found as a function of contact angle by insertion of equation (3.38) into equation (3.39). It depends only on the capacitance ratio C and the applied potential, and is independent of both b and $\cos\alpha_c^0$. Figure 4 shows $\phi_*/\Delta\phi$ as a function of contact angle and potential for the case where $C = 1.225$—typical of a 0.01 M nitrobenzene-solvated droplet, surrounded by a 0.01 M aqueous solution, at room temperature. In the figure, potential has been expressed dimensionally to make its order of magnitude clearer. As the figure shows, the partitioning of potential to the droplet bulk decreases monotonically with increasing contact angle. However, as the potential drop increases, the partition factor does as well. Moreover, as potential increases, ϕ_* stays near its maximum over an increasingly broad range of angles. The maximum values of the partition factor in the limits of small and large potentials are

$$\lim_{\Delta\phi\ll 1}\frac{\phi_*}{\Delta\phi} = \frac{C^4+1}{C^4+C^2+1} \qquad \text{and} \qquad \lim_{\Delta\phi\gg 1}\frac{\phi_*}{\Delta\phi} = \frac{2}{3}\left(1-\frac{2\ln C}{\Delta\phi}\right). \tag{3.41}$$

Thus, at very low potentials the partitioning is determined mainly by C. At large potentials, the partition factor asymptotically approaches a maximum of 2/3, as seen in figure 4.

Last let us briefly discuss b, which scales the impact of electrostatic action relative to that of capillary action. Figure 5 shows the contact-angle response and $\Phi_*/\Delta\Phi$ as a function

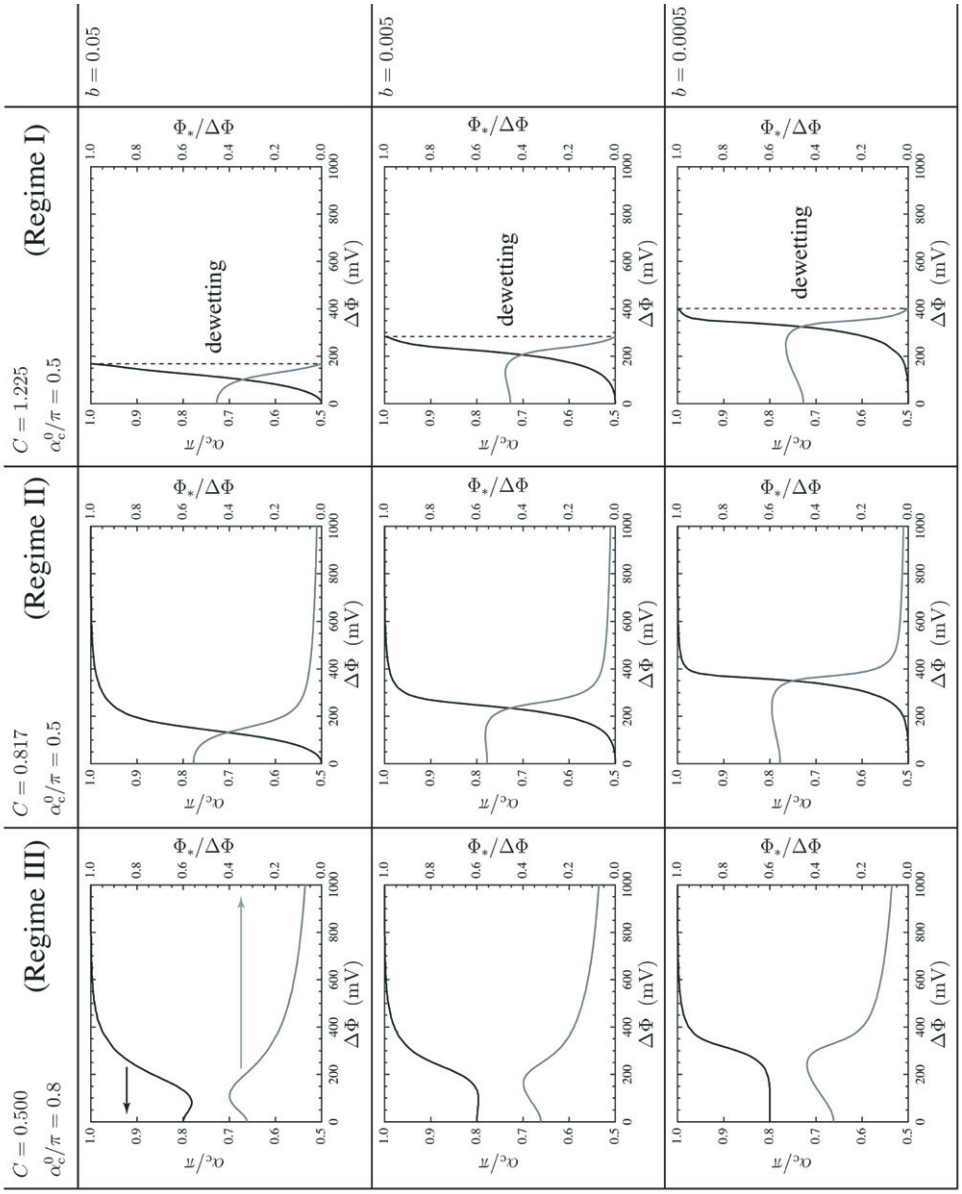

Figure 5. Contact angle, α_c, and partition potential, $\Phi_*/\Delta\Phi$, plotted as a function of $\Delta\Phi$ for electrowetting with an ITIES. In rows from top to bottom, values of C and α_c^0 correspond to regimes I, II and III on figure 3. In columns moving right, $b = 0.05$, 0.005 and 0.0005.

of applied potential. Nine combinations of C, α_c^0 and b are shown. Values of C and α_c^0 are chosen to correspond to each of the three regimes on figure 3; the contact-angle responses in these regimes are then plotted for three different orders of magnitude for b. More dramatic contact-angle response occurs with the same potential if b is larger: to achieve greater changes of contact angle with the same potential, salt content can be increased in both liquids, or a surfactant added to lower the liquid/liquid surface tension.

4. Electrowetting with an ion-permeable interface

One may now ask: if a system could be constructed with two conductive liquids and a completely ion-permeable interface, what would its electrowetting response be? This can be answered based on the results of the preceding section, but first one must question exactly how such a system could be engineered.

Complete ionic permeability requires that the free energies of transfer for all ions are zero. Data from various sources for the transfer free energies of a number of ions, at water/nitrobenzene and water/1,2-dichloroethane interfaces, are summarized in [26]. The lowest energetic transfer costs are for nitrobenzene and water as solvents, with tetraethylammonium iodide (TEAI) dissolved in both solutions. (Even in this case, iodide has an appreciable free energy of transfer, ∼0.05 eV, but it is the anion with the lowest transfer energy for this solvent pair.)

Composition equilibrium for this system would also require that the chemical potential of the TEAI be equal in both phases. To prepare solutions for which this is the case, a fixed amount of TEAI could be added to a stirred emulsion of water and nitrobenzene, and the solution allowed to equilibrate. After stirring was ceased, the two liquids could be separated by decanting. To establish their equilibrium concentrations, the densities of the decanted solutions could be compared to independent measurements of the density as a function of concentration.

Considerations like the above would be *necessary* to eliminate charge accumulation at the droplet/surroundings interface. None of these experimental requirements have been met for existing electrowetting systems, be they ones with ITIES or with one insulating fluid. Neither would such a system be easy to realize in practice. It is therefore surprising that charge accumulation at the droplet/surroundings interface has not been given more attention in the literature.

If a suitable choice of mutually miscible salt, with negligible transfer free energy, existed, and if a suitable reference electrode could be constructed to be reversible to the salt, then an applied potential drop between the working and reference electrodes would induce no potential drop across the liquid/liquid interface[7]. The contact-angle response would be given as a function of potential by

$$\cos\alpha_{\mathrm{c}} = \cos\alpha_{\mathrm{c}}^{0} - 8b\left(C - \tfrac{1}{C}\right)\sinh^{2}\left(\tfrac{1}{4}\Delta\phi\right). \tag{4.1}$$

This result is obtained simply by discarding the charge-constraint equation (3.39), setting ϕ_* to zero, and using equation (3.38) to replace A in equation (3.40).

This expression only yields two regimes of contact-angle response, which are shown on the phase diagram in figure 6, drawn for comparison to figure 3. Of course, the solution hardly merits a phase diagram, because the response predicted by the equation is independent of both α_{c}^{0} and b. If $C > 1$ (the surroundings have a higher Gouy–Chapman capacitance than the droplet), the droplet will contract until it dewets. If $C < 1$, the droplet expands until it completely covers the electrode surface.

Figure 7 gives characteristic curves for α_{c} versus potential. Note that the inflection points exhibited by all the curves on figure 5 are absent. The absence of inflection points is at variance with experimental observations, in which contact-angle saturation is typical [4].

The mutually opposed double layers which arise inside an electrolytic droplet have been overlooked in the past. This essential feature of electrowetting physics should also be

[7] For there to be no potential drop across the liquid/liquid interface, both ions must have transfer free energies *exactly* equal to zero. Note: if the free energies of transfer for both ions are truly zero, and both electrolytic solutions are truly ideal, then the equilibrium salt concentrations in both solutions have to be equal, and C differs from 1 only because the solvents have different dielectric constants.

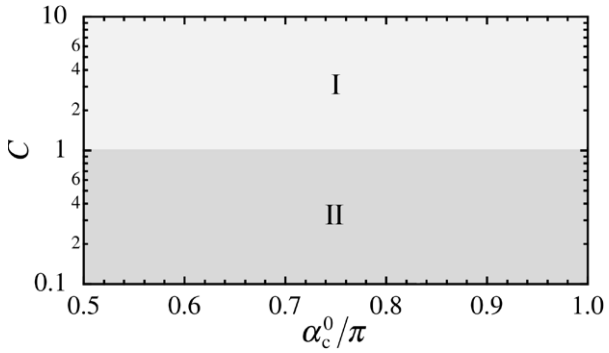

Figure 6. Characteristic responses of α_c to rising $\Delta\phi$ for an ion-permeable interface in a system with two mutually miscible salts, plotted as a phase diagram in the C/α_c^0 plane, with $b = 0.005$. (I) Angle rises monotonically until dewetting. (II) Angle falls monotonically until the droplet completely wets the electrode. This trivial picture is shown only for comparison to figure 3.

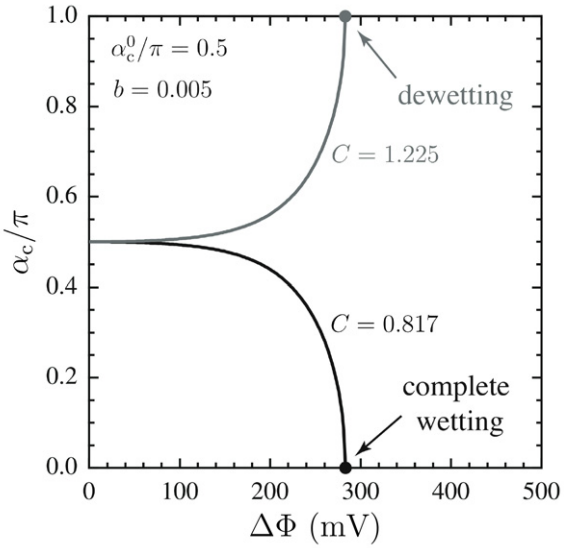

Figure 7. Contact angle, α_c, plotted as a function of $\Delta\Phi$ for electrowetting in a hypothetical system with a completely ion-permeable interface such that $b = 0.005$ and $\cos\alpha_c^0 = 0$. The grey curve, for $C = 1.225$, corresponds to regime I on figure 6; the black curve, for $C = 0.817$, corresponds to regime II.

included in the theoretical treatment of electrolytic droplets surrounded by pure-dielectric fluids. However, since a solution to this problem requires solution of Laplace's equation (rather than the Poisson–Boltzmann equation) in the surroundings, and the surroundings do not have an analytically tractable shape, this important case is left for future work, perhaps by numerical simulation. However, for a majority of applications, electrowetting systems with one conductive and one nonconductive fluid can be replaced with ITIES, which offer much finer control of contact angles at much lower voltages.

5. Conclusion

Our group has worked on different aspects of the theory of ITIES for the last decade [11, 19]. Two years ago, inspired by a suggestion of Hubert Girault (EPFL), we focused attention on three-phase systems consisting of an ITIES adjacent to a metal electrode. The initial motivation was to understand the potential distribution near the three-phase boundary—a potentially important question for electrocatalysis.

Field divergence near the three-phase line is a major concern in familiar liquid/liquid electrowetting systems, which involve an interface between one conductive and one insulating fluid [20]. Frustrating characteristics of the contact-angle response in these systems have been attributed to this phenomenon, which is difficult to model [5]. Our investigation of the electrostatics of ITIES showed, in contrast, that at experimentally accessible length scales, no dramatic effects arise from the potential distribution near a three-phase line. This led unexpectedly to the discovery of a new, ITIES-based electrowetting system [6].

This article develops our first paper, which was limited to electrowetting with ITIES at small applied voltages [6], by extending the theory—within stated limitations of the model—to arbitrarily large voltages. It comprises a detailed analysis of the problem, a few main results of which were highlighted in an earlier letter [7]. Here we have (i) presented all aspects of the derivational procedure needed to formulate and solve the electrostatic problem, and to obtain contact angles as a function of electrode potential, (ii) displayed a complete set of results for ITIES, which was not possible in the previous brief communication, and (iii) presented additional results for electrowetting systems with two ionically conductive fluids, but where the liquid/liquid interface is ion-permeable.

We unambiguously show that the ITIES-based electrowetting system allows very fine control of the contact-angle response to potential, and can operate at voltages 10–100 times smaller than those needed in currently existing devices [21]. Preliminary experiments have been performed by Alice Sleightholme and Anthony Kucernak at Imperial College London, which basically confirm the theoretical predictions [22]. These observations will be reported elsewhere.

Along with the advantage of low-potential operation, electrowetting with ITIES allows a relatively simple closed-form theoretical description. The system response depends primarily on three parameters, which are determined explicitly by properties of the two electrolytic solutions and the electrode substrate. In addition to enhancing physical insight, this suggests a concise set of control variables for the experimental analysis of more complicated systems.

Although it may not be practically possible to realize, the case of an ion-permeable liquid/liquid interface has its own merits. The results illustrate what may happen to an ITIES at large voltages, which can compensate the free energies of transfer and induce ion penetration through the liquid/liquid interface. The natural expectation would be that when a field induces penetration, the electrowetting curve might abruptly transition to dewetting or complete wetting of the electrode, with the direction of the transition determined by electrolyte composition. Of course this large-voltage regime requires more rigorous analysis, which will be provided elsewhere.

Also, the experimental setup was discussed in detail and a number of issues concerning the counter and/or reference electrodes were brought to light. These subtleties have not been discussed before in the electrowetting literature, although ignoring them can lead to inexplicable discrepancies between theory and experiments.

Last, but not least, it should be emphasized that ITIES-based electrowetting systems have great potential for additional functionalization. Both adsorption phenomena and chemical reactivity can be controlled by the applied voltage, with the effects highly localized near the

liquid/liquid interface [23, 24]. This opens new avenues by which to alter the optical and sensing properties within electrowetting devices.

Acknowledgments

The authors are grateful to Leonid Daikhin (Tel Aviv University, Ramat Aviv), Hubert Girault (EPFL, Lausanne), Anthony Kucernak (Imperial College London), Sasha Kuznetsov (Frumkin Institute, Moscow) and Alice Sleightholme (Imperial College London). This work was supported by the Leverhulme Trust, Interchange Grant no. F/07058/P, and the Israel Science Foundation, grant no. 773/05. AAK also acknowledges the Royal Society Wolfson Merit Research Award.

Appendix. Properties of electrolytes with impermeable boundaries: basic concepts

A.1. Free energies of transfer and the ideal polarizability window

One key feature of electrowetting systems which have a dissolved salt in the droplet phase is that the droplet/surroundings interface may be impermeable to ions over a large potential range. Consider a case where the droplet consists of a solution of sodium chloride in water, and the surroundings are a nonpolar solvent, such as high-molecular-weight silicone oil. (Experimental data for this electrowetting system are presented in the review article by Mugele and Baret [4].) In this case, the sodium chloride has extremely low solubility in the silicone; the salt remains in water, where it is most comfortably solvated.

Even when a potential bias is applied, inducing a field to 'push' anions or cations, ions tend to stay in the phase where they are well solvated. The amount of energy required for the ions to change phases, i.e. to discard a solvation shell of one type of solvent and exchange it entirely for another, is called the *free energy of transfer*. Typically, because immiscible fluids have very different polarity, the differences in their ionic solvation energies—and thus their free energies of transfer—are large. For instance, for aqueous sodium chloride, the free energies of transfer for Na^+ or Cl^- into nitrobenzene are of order 0.3 eV; the magnitudes are similar for transfer of tetrabutylammonium (TBA^+) or tetraphenylborate (TPB^-) from nitrobenzene into water.

When free energies of transfer are high, the potential drop needed to induce ion exchange is also high: the interface acts as 'ion-impermeable' over a broad potential range. This range can be determined by cyclic voltammetry; it commonly extends from zero bias up to a bias of 500 mV, and can sometimes go significantly higher than a volt.

Transfer free energies have been measured in abundance, particularly for interfaces of aqueous solutions with nitrobenzene, dichloroethane and similar organic solvents [25, 26]. Since in these cases free energies of transfer for alkali halides are large, one would presume that the same is the case for the aqueous NaCl/silicone oil interface, more typical of conventional electrowetting systems. For an electrolyte/air interface (that is, if the surrounding fluid is air), one would imagine that ionic free energies of transfer would be still higher.

The range of potentials within which there is no Faradaic current across an interface is called the regime of *ideal polarizability* [27]. At an ITIES, ideal polarizability implies that there is no ionic current across the interface. At a metal/electrolyte interface, it implies the absence of Faradaic currents, such as those arising from electron-transfer reactions between the electrode and dissolved ions. In this work all the interfaces with solids are taken to be ideally polarizable[8].

[8] High enough voltages can always trigger electrochemical reactions at an interface. However, many metal electrodes have a several-hundred millivolt window of ideal polarizability, the width of which can be assessed by cyclic voltammetry; ITIES have also been observed to behave as if they are ideally polarizable over several hundred millivolts [15].

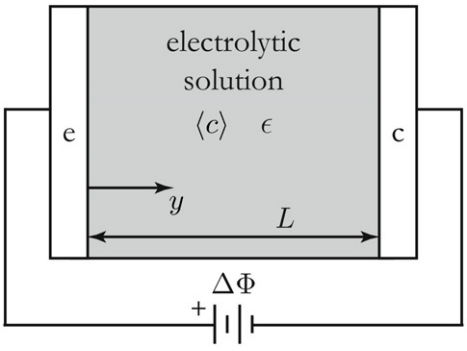

Figure A.1. Schematic of a parallel-plate double-layer capacitor with plate separation L along the y-axis. The fluid between plates has dielectric constant ϵ; the average electrolyte concentration is $\langle c \rangle$. Between the working and counterelectrodes a potentiostat maintains potential drop $\Delta\Phi$.

A.2. Double layers in a confined volume of electrolytic solution which conserves its contents: tutorial example

What happens to an electrolytic phase bounded by ideally polarizable interfaces when a potential drop is applied across it? The answer can be illustrated with the functional developed in section 2. Although the following discussion looks somewhat tangential to electrowetting, it is not: it provides a convenient illustration of how ideally polarizable boundaries affect the electrostatic response of electrolytic phases, in general.

Consider the one-dimensional parallel-plate double-layer capacitor sketched in figure A.1. In this case there is only one fluid phase; the pressure is held constant, and, because the electrolytic solution remains in contact with a fixed electrode area, $\mathscr{C}$ is constant and does not affect the position of the free-energy minimum. For simplicity the electrolyte is taken to be symmetric, with ionic equivalent charges $z_+ = -z_- = z$; it is also assumed that each formula unit of the salt contains only a single cation and a single anion (i.e. the salt has 1:1 stoichiometry). The electrodes of the capacitor are taken to be ideally polarizable and smooth on molecular dimensions. A potentiostat applies a potential difference between phases e and c.

This system has been selected for the sole reason that the geometry is simple, there is only one fluid phase, and *the system boundaries are impermeable to ions*—a condition which often holds at the boundaries of electrolytic droplets in electrowetting.

Derivation of governing equations from the functional—If the electrolytic solution is ideal, the appropriate form for $\mathscr{W}$ is

$$\mathscr{W} = RTA \int_0^L c_\mathrm{T} \left(x_0 \ln x_0 + x_+ \ln x_+ + x_- \ln x_-\right) \mathrm{d}y + A \int_0^L \rho\Phi \, \mathrm{d}y, \quad \text{(A.1)}$$

A being the surface area of the parallel electrodes, and subscripts 0, + and − corresponding to solvent, cations and anions in the electrolytic solution, respectively; here c_T is the total molar concentration of the solution. The overall functional G is obtained by adding $\mathscr{V}$ from equation (2.3) to the above and incorporating the electrostatic potential through $\mathbf{E} = -\nabla\Phi$. Equilibrium is achieved when G is at a minimum with respect to the distributions of potential and every species concentration.

As is clear from the fact that the interior of the parallel-plate capacitor is a closed system, minimization of the functional must be performed under several constraints. The total charge Q between plates is zero; also, the number of solvent molecules, N_0, and the number of ions

present, N_+ and N_-, cannot change because the fluid's boundaries are ideally polarizable. Thus

$$Q = A\int_0^L \rho\,\mathrm{d}y, \qquad N_0 = A\int_0^L c_\mathrm{T} x_0\,\mathrm{d}y, \qquad \text{and} \qquad N_\pm = A\int_0^L c_\mathrm{T} x_\pm\,\mathrm{d}y \tag{A.2}$$

must all remain constant. (Although clearly $Q = Fz(N_+ - N_-)$, and the charge is obviously zero, it will be convenient to use Q as a Lagrangian constraint, set to zero later in the calculation.) The functional to be varied is then

$$\frac{G}{A} = RT\int_0^L c_\mathrm{T}\left(x_0\ln\frac{x_0}{x_0^\mathrm{ref}} + x_+\ln\frac{x_+}{x_+^\mathrm{ref}} + x_-\ln\frac{x_-}{x_-^\mathrm{ref}}\right)\mathrm{d}y + \int_0^L \rho(\Phi-\Phi_*)\,\mathrm{d}y - \frac{\epsilon_0}{2}\int_0^L \epsilon\nabla\Phi\cdot\nabla\Phi\,\mathrm{d}y, \tag{A.3}$$

where x_i^ref are Lagrange multipliers which allow satisfaction of the constraints on N_0, N_+ and N_-; Φ_* permits application of the constraint on Q.

Typically solutes have a much lower concentration than the solvent in electrolytic solutions. If the solution is dilute, then because $\sum_i x_i^\mathrm{ref} = 1$,

$$x_+ + x_- \ll 1, \qquad x_+^\mathrm{ref} + x_-^\mathrm{ref} \ll 1, \qquad \text{and} \qquad c_\mathrm{T} \approx c_0 = \text{constant}, \tag{A.4}$$

where the latter conditions follow from the first, as well as equations (2.6) and (A.2). Assuming that ϵ is also constant, the free energy functional can be expressed per unit electrode area as

$$\frac{G}{A} = RT\int_0^L \left[c_+\left(\ln\frac{c_+}{c_\mathrm{b}} - 1\right) + c_-\left(\ln\frac{c_-}{c_\mathrm{b}} - 1\right) + 2c_\mathrm{b}\right]\mathrm{d}y + \int_0^L \rho(\Phi-\Phi_*)\,\mathrm{d}y - \frac{\epsilon_0\epsilon}{2}\int_0^L \nabla\Phi\cdot\nabla\Phi\,\mathrm{d}y, \tag{A.5}$$

where the identity $c_i = x_i c_\mathrm{T}$ has been used to express the result in terms of concentrations. The bulk salt concentration c_b is defined here by

$$c_\mathrm{b} = c_\mathrm{T} x_+^\mathrm{ref} = c_\mathrm{T} x_-^\mathrm{ref}, \tag{A.6}$$

appropriate because the electrolyte is 1:1 ($N_+ = N_-$, and either equals the total number of dissolved salt formula units). Asymmetric electrolytes could be treated by adding stoichiometric coefficients here; these only serve to complicate the algebra and have been avoided for brevity.

Functional (A.5) can be varied with Φ, c_+, and c_- to obtain equations governing the potential and ion-concentration distributions inside the capacitor. Take the variation of G with respect to each ion-concentration distribution, with the potential and the remaining ion concentration fixed, and equate to zero, to find

$$c_\pm = c_\mathrm{b}\exp\left[\mp\frac{zF(\Phi-\Phi_*)}{RT}\right]; \tag{A.7}$$

the ions are Boltzmann distributed in the potential relative to Φ_*.[9] Note that c_b, which is the concentration of anions or cations at $\Phi = \Phi_*$, remains to be found self-consistently through the Lagrangian constraints; Φ_* must also be found self-consistently, as described below.

The variation of G with respect to potential, with both ion concentrations fixed, shows

$$\nabla^2(\Phi-\Phi_*) = -\frac{Fz}{\epsilon_0\epsilon}(c_+ - c_-), \tag{A.8}$$

[9] If the dilute-solution approximation had been avoided, Fermi-like distributions would arise here [28]. These distributions would be parameterized by the partial molar volumes which appear in equation of state (2.6).

i.e. that the potential obeys Poisson's equation. Variation with Φ also yields a condition on **E**—the charges on the surfaces of the capacitor plates must be equal and opposite, consistent with the condition $Q = 0$ through Gauss's law. In light of equations (A.7) and (A.8), Φ obeys a nonlinear Poisson–Boltzmann equation within the electrolytic solution, where the 'bulk potential' Φ_* is chosen so that the solution accumulates no total charge.

Given that the electrolyte is dilute, symmetric and 1:1, the constraints can be simplified significantly. The solvent concentration changes negligibly in the dilute-solution approximation; the constraint on N_0 becomes trivial and can be discarded. Also, since $Q = Fz(N_+ - N_-)$, any one of the three remaining constraints depends linearly on the others. Last, the average concentration (an experimentally fixed system parameter) relates to the molar contents of cations and anions through $\langle c \rangle = \frac{1}{2}(N_+ + N_-)/AL$. To find the two Lagrange multipliers Φ_* and c_b, one only needs to solve

$$\int_0^L \sinh\left[\frac{zF\,(\Phi - \Phi_*)}{RT}\right] \mathrm{d}y = 0 \tag{A.9}$$

on Φ_*, and substitute into

$$\frac{1}{L}\int_0^L \cosh\left[\frac{zF\,(\Phi - \Phi_*)}{RT}\right] \mathrm{d}y = \frac{\langle c \rangle}{c_\mathrm{b}} = \frac{1}{\chi^2} \tag{A.10}$$

to find c_b. These simplified versions of equations (A.2) also incorporate the Boltzmann distributions from equation (A.7). The first expresses the charge constraint and the second that the average salt concentration, $\langle c \rangle$, is fixed. Note the second equation also introduces the convenience parameter χ, related to the ratio of the average and bulk concentrations by $\chi \equiv \sqrt{c_\mathrm{b}/\langle c \rangle}$.

Thus arises a novel feature of an electrolytic phase with ion-impermeable boundaries: the *average* concentration of the salt, $\langle c \rangle$ (the total number of salt formula units divided by the solution volume) does not necessarily equal the *bulk* concentration of the salt, c_b (the local salt concentration in a region where $\Phi = \Phi_*$). When a potential bias is applied, anions are drawn toward a positive potential, and cations toward a negative one—consequently the total electrolyte concentration in the centre of the capacitor is depleted. Equation (A.10) supports this conclusion. Hyperbolic cosines have the minimum value 1. Therefore, if the constraint in equation (A.10) is to be satisfied, then $\chi \leqslant 1$ and $c_\mathrm{b} \leqslant \langle c \rangle$ for any $\Phi(y)$.

By insertion of equation (A.7) into (A.8), one obtains

$$\frac{1}{(\chi\kappa)^2}\nabla^2\left[\frac{zF\,(\Phi - \Phi_*)}{RT}\right] = \sinh\left[\frac{zF\,(\Phi - \Phi_*)}{RT}\right], \tag{A.11}$$

where the inverse Debye length κ is given its familiar definition, in terms of the average concentration $\langle c \rangle$, as

$$\kappa = \sqrt{\frac{2F^2z^2\,\langle c \rangle}{\epsilon_0 \epsilon RT}}. \tag{A.12}$$

Equation (A.11) is identical to the familiar nonlinear Poisson–Boltzmann equation except for the presence of the parameter χ. It can be concluded that when a potential drop is applied, depletion of the salt at $\Phi = \Phi_*$, which occurs because $\chi \leqslant 1$, leads to an effective increase in Debye length.

A.3. Solution for small voltages

Imagine that the bias is maintained sufficiently low that $\Phi - \Phi_*$ is everywhere small[10]. Equation (A.11) can be approximated as

$$\nabla^2 \left[\frac{zF\,(\Phi - \Phi_*)}{RT} \right] \approx (\chi\kappa)^2 \frac{zF\,(\Phi - \Phi_*)}{RT} + \mathrm{O}\left[(\Phi - \Phi_*)^3\right], \tag{A.13}$$

where it should be noted that the next correction is of third order. Up to third order in potential, the charge constraint becomes

$$0 = \frac{zF}{RT} \int_0^L (\Phi - \Phi_*)\ \mathrm{d}y + \mathrm{O}\left[(\Phi - \Phi_*)^3\right], \tag{A.14}$$

and the constraint on salt content is

$$1 - \frac{1}{\chi^2} = \frac{1}{2L} \left(\frac{zF}{RT} \right)^2 \int_0^L (\Phi - \Phi_*)^2\ \mathrm{d}y + \mathrm{O}\left[(\Phi - \Phi_*)^3\right]. \tag{A.15}$$

This completes the development of governing equations for the capacitor in the regime of quadratic potential response.

The potential drop between the capacitor's electrodes is fixed by the potentiostat; the electrodes themselves are equipotential surfaces. To determine the potential distribution, equation (A.13) is solved with the following boundary conditions on $\Phi(y)$:

$$\Phi(0) = \Phi_\mathrm{e} \qquad \text{and} \qquad \Phi(L) = \Phi_\mathrm{c}. \tag{A.16}$$

In the quadratic regime, the potential distribution is

$$\Phi - \Phi_* = \frac{\Delta\Phi \sinh\left[\frac{1}{2}\chi\kappa(L - 2y)\right]}{2\sinh\left(\frac{1}{2}\chi\kappa L\right)} + \mathrm{O}(\Delta\Phi^3), \tag{A.17}$$

where $\Delta\Phi \equiv \Phi_\mathrm{e} - \Phi_\mathrm{c}$. The two constraint conditions, equations (A.14) and (A.15), become

$$\begin{aligned} \Phi_* &= \frac{\Phi_\mathrm{e} + \Phi_\mathrm{c}}{2} + \mathrm{O}(\Delta\Phi^3), \\ \frac{\kappa L(1 - \chi^2)\tanh\left(\frac{1}{2}\chi\kappa L\right)}{\chi\left[1 - \frac{\chi\kappa L}{\sinh(\chi\kappa L)}\right]} &= \frac{1}{8}\left(\frac{zF\Delta\Phi}{RT}\right)^2 + \mathrm{O}(\Delta\Phi^3). \end{aligned} \tag{A.18}$$

The bulk potential Φ_* takes an intermediate value between the potentials at either electrode. It can be seen from the second equation that $\chi \to 1$ as $\Delta\Phi \to 0$ and $\chi \to 0$ as $\Delta\Phi \to \infty$.

The surface-charge density in the electrolytic solution immediately adjacent to the electrodes can also be obtained from the potential distribution in equation (A.17),

$$\sigma_{y=0} = \epsilon_0\epsilon\nabla\Phi|_{y=0} = -\epsilon_0\epsilon\nabla\Phi|_{y=L} = -\frac{\epsilon_0\epsilon\chi\kappa\Delta\Phi}{2\tanh\left(\frac{1}{2}\chi\kappa L\right)} = -\sigma_{y=L}. \tag{A.19}$$

Of course the surface-charge densities are equal and opposite, as is expected because $Q = 0$ and both electrodes have the same area.

Concentration and potential distributions for three capacitors with $\Delta\Phi = 50$ mV are shown in figure A.2. Three lengths are shown: $\kappa L = 2.5$, 5 and 10. The figure shows that charge is screened over a smaller fraction of the capacitor interior as length increases (moving down in the figure). Note that in the lower plots a potential plateau near Φ_* begins to form at the centre of the capacitor, and 'separate' double layers start to form near both electrodes.

[10] The nonlinear case could be treated with some additional analytical gymnastics. However, the analytical equations are more easily interpreted in the small-potential regime. Suffice it to say that the main conclusions of this work rely mainly on approximation (A.21). For nonlinear cases, κ is replaced with $\kappa\cosh(zF\Delta\Phi/2RT)$ (the Debye-length contraction from nonlinear Gouy–Chapman theory [12, 13]). This can be inserted into equation (A.21) to show that the condition is overly conservative outside the quadratic potential regime.

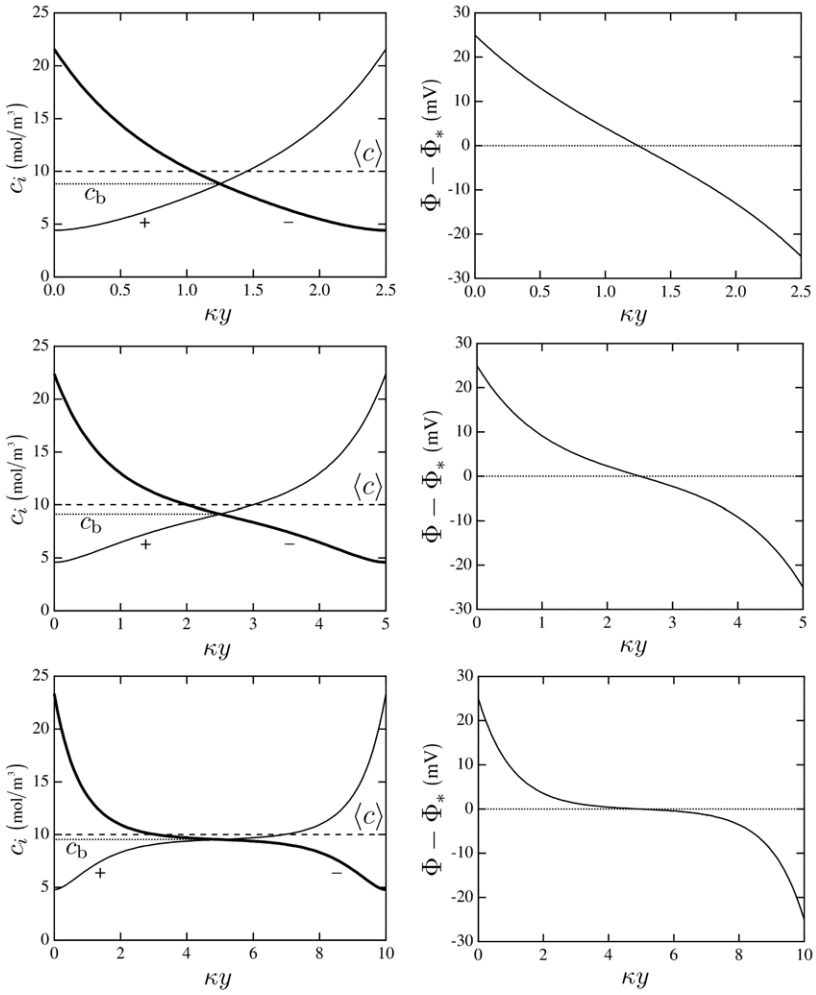

Figure A.2. Concentration and potential distributions in parallel-plate double-layer capacitors with $\Delta\Phi = 50$ mV, for cases when $\kappa L = 2.5$, 5, and 10.

Limiting cases—It is also instructive to explore certain limits of equations (A.17) and (A.18). When $\kappa L \to 0$:

$$\lim_{\kappa L \to 0} (\Phi - \Phi_*) = \Delta\Phi \left(\frac{1}{2} - \frac{y}{L} \right) \qquad \text{and} \qquad \lim_{\kappa L \to 0} \sigma_{y=0} = -\epsilon_0 \epsilon \frac{\Delta\Phi}{L}. \tag{A.20}$$

These are familiar equations for parallel-plate dielectric capacitors. When the Debye length is very long compared to the characteristic size of the phase, an electrolytic solution with impermeable boundaries behaves like a pure-dielectric medium. The plot with $\kappa L = 2.5$ in figure A.2 shows the approach to this regime; because the cell length is of the order of the Debye length, the potential distribution is nearly linear.

Of course, the case of small κ is not applicable to typical electrolytic solutions, where $1/\kappa$ tends to represent a length scale of nanometres or angstroms. However, this limit does show that the functional approach yields satisfactory limiting behaviour.

Each of the graphs in figure A.2 shows conditions with the same potential drop $\Delta\Phi$. As the capacitor gets longer (as κL increases), the bulk concentration approaches the average

concentration. It is worthwhile to learn the potential range where the approximation $c_b \approx \langle c \rangle$ is valid. Perturbation of the second of equations (A.18) gives

$$\chi \approx 1 \qquad \text{when } |\Delta\Phi| \ll \frac{4RT}{zF}\sqrt{\kappa L \tanh\left(\frac{1}{2}\kappa L\right)}. \tag{A.21}$$

At room temperature, the prefactor on the square root is about 100 mV. Thus, in a closed electrolytic phase at ambient temperature, the concentration at Φ_* can be taken to equal the average salt concentration over a ± 3 V window when $\kappa L = 1000$. As κL increases, so does the size of the voltage window. In short: $\chi \approx 1$ is an extremely good approximation, as the neglected Faradaic processes typically begin well below 3 V.

It is most instructive to consider very large values of κL, more typical of ordinary electrochemical experiments. In this regime (also taking $\chi \approx 1$, on the basis of equation (A.21)), the distribution of potential simplifies to

$$\lim_{\kappa L \gg 1}(\Phi - \Phi_*) = \frac{\Delta\Phi}{2}\left\{\exp(-\kappa y) - \exp\left[-\kappa L\left(1 - \frac{y}{L}\right)\right]\right\}, \tag{A.22}$$

or, examining the result near either electrode,

$$\begin{aligned} &\lim_{\kappa L \gg 1}(\Phi - \Phi_*) = \frac{\Delta\Phi}{2}\exp(-\kappa y); \qquad \frac{y}{L} \ll 1, \\ &\lim_{\kappa L \gg 1}(\Phi - \Phi_*) = -\frac{\Delta\Phi}{2}\exp[-\kappa(L - y)]; \qquad \left(1 - \frac{y}{L}\right) \ll 1. \end{aligned} \tag{A.23}$$

These show that when the capacitor is very large compared to the Debye length, the interfaces each form linear Gouy–Chapman-like double layers. This is another validation of the constrained Lagrangian approach developed here: for large systems, it leads to conclusions in precise agreement with those deduced from the semi-infinite linear Poisson–Boltzmann theory.

However, for the parallel-plate double-layer capacitor, an important result differs from the standard semi-infinite treatment. Consider the surface charges at the capacitor plates. When $\kappa L \gg 1$, the surface-charge densities become

$$\sigma_{y=0} = -\frac{\epsilon_0 \epsilon \kappa \Delta\Phi}{2} = -\sigma_{y=L}. \tag{A.24}$$

In the capacitor, the constraints on total ion content require that surfaces maintain equal and opposite charges, even when κL is extremely large. Also note that differentiation of $-\sigma_{y=0}$ with respect to $\Delta\Phi$ yields a capacitance which corresponds to two linear Gouy–Chapman capacitances in series, as one would expect.

If the above analysis is performed without the approximation of small $\Delta\Phi$, the principal conclusions agree with the results Gouy and Chapman obtained from *nonlinear* Poisson–Boltzmann theory for semi-infinite systems [12, 13]. The parallel-plate double-layer capacitor yields two nonlinear Gouy–Chapman capacitances in series, while Φ_* remains the average of the electrode potentials.

A.4. Working principles

In the main body of this paper, nonlinear effects are considered in detail for electrowetting with electrolytes. Several qualitative conclusions can be drawn from the previous example, which apply equally in the linear- and nonlinear-response regimes.

(1) Due to the impermeability of its boundaries, a closed electrolytic phase contains fixed numbers of ions and solvent molecules. Consequently the interior of the phase has zero net charge, even when a potential drop is applied across it.

(2) If an electrolytic phase has an ion-impermeable surface, and has dimensions on the order of its Debye length, then its electrostatic response at low potentials will be similar to that of a purely dielectric medium.
(3) If a closed electrolytic phase has a characteristic size much greater than its Debye length, double layers will form in its interior. However, these double layers appear in such a way that the surface charges on the phase boundaries sum to zero. Thus, for an electrolytic droplet with high ionic free energies of transfer, there are space-charge regions at both the droplet/electrode interface *and* the interface between the droplet and its surrounding fluid (see figure 1). Overall electroneutrality of the droplet results in equal and opposite space charges within the double layers at these two boundaries.
(4) If an electrolytic droplet has impermeable boundaries and is much larger than its Debye length, a plateau near the bulk potential Φ_* extends over most of its interior; Φ_* is between the potentials at the electrode/droplet and droplet/surroundings interfaces.
(5) In closed electrolytic phases the formation of balanced double layers depletes the electrolyte concentration at Φ_*, c_b, below the average electrolyte concentration $\langle c \rangle$. This change can be neglected, $c_b \approx \langle c \rangle$, over the range of experimentally accessible potentials when the scale of the phase is greater than 1000 Debye lengths.

There are two other important qualitative aspects of electrowetting phenomena which have already been discussed at length in earlier work [6]:

(1) In electrowetting systems with an electrolytic droplet and electrolytic surroundings, the potential is nearly constant across the entire droplet/surroundings interface, even when this interface is curved. The droplet/electrode and droplet/surroundings interfaces are essentially equipotential surfaces, obeying boundary conditions like the capacitor plates did in the previous example. The potential at the droplet surface varies only in a region that extends fewer than two Debye lengths from the three-phase contact line.
(2) In electrowetting systems with an electrolytic droplet and electrolytic surroundings, the potential distribution very near the three-phase contact line contributes negligibly to the total free energy when the scale of the droplet is greater than 1000 Debye lengths.

References

[1] Berge B and Peseux J (inventors) 1999 Lens with variable focus *World Intellectual Property Organisation* no. 9918456, Univ. Joseph Fourier, France
Berge B, Peseux J, Boutaud B and Craen P (inventors) 2006 Variable-focus lens assembly *World Intellectual Property Organisation* no. WO 2006/136612, Varioptic, France
[2] Boutet J (inventor) 2007 Microfluidic device for measuring fluorescence and measuring method using same, *World Intellectual Property Organisation* no. WO 2007/012637, Commissariat Energie Atomique, France
Pamula V K, Pollack M G, Paik P Y, Ren H and Fair R B (inventors) 2004 Methods and Apparatus for manipulating droplets by electrowetting-based techniques *US Patent Specifiation* 4058450 Jenkins and Wilson, PA, United States
[3] Clarke A (inventor) 2005 Electrowetting display element *World Intellectual Property Organisation* no. WO 2005/096066, Eastman Kodak Company, United States
Glass T R (inventor) 2007 Electrowetting display *US Patent Specification* 7167156 Micron Technology, Inc., United States
[4] Mugele F and Baret J-C 2005 Electrowetting: From basics to applications *J. Phys.: Condens. Matter* **17** R705–74
[5] Chou T 2001 Geometry-dependent electrostatics near contact lines *Phys. Rev. Lett.* **87** 106101
[6] Monroe C W, Daikhin L I, Urbakh M and Kornyshev A A 2006 Principles of electrowetting with two immiscible electrolytic solutions *J. Phys.: Condens. Matter* **18** 2837–69
[7] Monroe C W, Daikhin L I, Urbakh M and Kornyshev A A 2006 Electrowetting with electrolytes *Phys. Rev. Lett.* **97** 136102

[8] Girault H H and Schiffrin D 1985 Electrochemistry of liquid–liquid interfaces *Electroanalytical Chemistry* vol 1, ed A J Bard (New York: Dekker) pp 1–62
[9] Ivošević N and Žutić V 1998 Spreading and detachment of organic droplets at an electrified interface *Langmuir* **14** 231–4
[10] Guggenheim E A 1959 *Thermodynamics* (Amsterdam: North-Holland)
[11] Monroe C W, Urbakh M and Kornyshev A A 2005 Understanding the anatomy of capacitance at interfaces between two immiscible electrolytic solutions *J. Electroanal. Chem.* **582** 28–40
[12] Gouy G L 1910 Sur la consitution de la charge électrique a la surface d'un électrolyte *J. Physiol.* **9** 457–68
[13] Chapman D L 1913 A contribution to the theory of electrocapillarity *Phil. Mag.* **25** 475–81
[14] Verwey E J W and Niessen K F 1939 The electrical double layer at the interface of two liquids *Phil. Mag.* **28** 435–46
[15] Samec Z, Mareček V and Homolka D 1984 Double layers at liquid/liquid interfaces *Faraday Discuss. Chem. Soc.* **77** 197–208
[16] Safran S A 1994 *Statistical Thermodynamics of Surfaces, Interfaces, and Membranes* (Reading, MA: Addison-Wesley)
[17] Parsons R 1954 Equilibrium properties of electrified interphases *Mod. Aspects Electrochem.* **1** 103–79
[18] Kornyshev A A, Spohr E and Vorotyntsev M A 2002 Electrochemical interfaces: at the border line *Encyclopedia of Electrochemistry* vol 1 *Thermodynamics and Electrified Interfaces* ed E Gileadi and M Urbakh (Weinheim: Wiley–VCH) pp 33–132
[19] Regarding dynamic liquid/liquid interfacial morphology: Daikhin L I, Kornyshev A A and Urbakh M 2000 Capillary waves at soft electrified interfaces *J. Electroanal. Chem.* **483** 68–80
Kornyshev A A and Urbakh M 2004 Direct energy transfer at electrified liquid–liquid interfaces: a way to study interface morphology on mesoscopic scales *Electrochem. Commun.* **6** 703–7
Regarding ion transfer at ITIES: Kornyshev A A, Kuznetsov A M and Urbakh M 2002 Coupled ion-interface dynamics and ion transfer across the interface of two immiscible liquids *J. Chem. Phys.* **117** 6766–79
Verdes C G, Urbakh M and Kornyshev A A 2004 Surface tension and ion transfer across the interface of two immiscible electrolytes *Electrochem. Commun.* **6** 693–9
Daikhin L I, Kornyshev A A, Kuznetsov A M and Urbakh M 2005 ITIES fluctuations induced by easily transferable ions *Chem. Phys.* **319** 253–60
Regarding coupling of dynamic morphology and ion transfer at ITIES: Daikhin L I, Kornyshev A A and Urbakh M 2001 Ion penetration into an unfriendly medium and the double layer capacitance of the interface between two immiscible electrolytes *J. Electroanal. Chem.* **500** 461–70
[20] Berge B and Peseaux J 2000 Variable focal lens controlled by an external voltage: An application of electrowetting *Eur. Phys. J.* E **3** 159–63
[21] To see operational voltages for some devices on the market, link through Varioptic, at http://www.varioptic.com/en/index.php
[22] Sleightholme A E S and Kucernak A 2006 personal communication (Imperial College London)
[23] Girault H H 2006 Electrowetting: shake, rattle, and roll *Nat. Mater.* **5** 851–2
[24] Su B, Abid J-P, Fermín D J, Girault H H, Hoffmannová H, Krtil P and Samec Z 2004 Reversible voltage-induced assembly of Au nanoparticles at liquid–liquid interfaces *J. Am. Chem. Soc.* **126** 915–9
[25] Samec Z, Homolka D, Mareček V and Kavan L 1983 Charge transfer between two immiscible electrolyte solutions: transfer of tris(2,2′-bipyridine)ruthenium(ii) and alkyl viologen dications across the water/nitrobenzene, water/dichloromethane, and water/dichloroethane interfaces *J. Electroanal. Chem.* **145** 213–8
[26] For a review see: Kornyshev A A and Volkov A G 1984 On the evaluation of standard Gibbs energies of ion transfer between two solvents *J. Electroanal. Chem.* **180** 363–81
[27] Newman J and Thomas-Alyea K E 2004 *Electrochemical Systems* 3rd edn (New Jersey: Wiley)
[28] Borukhov I, Andelman D and Orland H 2000 Adsorption of large ions from an electrolyte solution: a modified Poisson–Boltzmann equation *Electrochim. Acta* **46** 221–9